

**UNIVERSIDADE FEDERAL DE SANTA CATARINA
PROGRAMA DE PÓS-GRADUAÇÃO EM ENGENHARIA
ELÉTRICA**

Thiago de Alencar Sousa

**HANDLING THE STOCHASTIC HYDROTHERMAL UNIT
COMMITMENT WITH DIFFERENT MODELS OF PIECEWISE
LINEAR HYDROPOWER PRODUCTION FUNCTIONS**

Florianópolis
2018

Thiago de Alencar Sousa

**HANDLING THE STOCHASTIC HYDROTHERMAL UNIT
COMMITMENT WITH DIFFERENT MODELS OF PIECEWISE
LINEAR HYDROPOWER PRODUCTION FUNCTIONS**

Master's Thesis submitted to the Post-graduation Program in Electrical Engineering of the Federal University of Santa Catarina to obtain the degree of Master in Electrical Engineering.
Advisor: Prof. D. Eng. Erlon Cristian Finardi

Florianópolis
2018

Ficha de identificação da obra elaborada pelo autor,
através do Programa de Geração Automática da Biblioteca Universitária da UFSC.

Sousa, Thiago de Alencar
Handling the Stochastic Hydrothermal Unit
Commitment with different models of piecewise
linear Hydropower Production Functions / Thiago de
Alencar Sousa ; orientador, Erlon Cristian
Finardi, 2018.
104 p.

Dissertação (mestrado) - Universidade Federal de
Santa Catarina, Centro Tecnológico, Programa de Pós
Graduação em Engenharia Elétrica, Florianópolis, 2018.

Inclui referências.

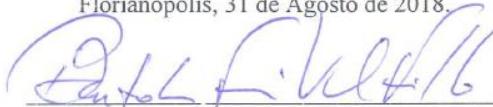
1. Engenharia Elétrica. 2. Unit Commitment
problem. 3. Hydro Production Function. 4. Two-stage
stochastic programming. 5. Benders Decomposition.
I. Cristian Finardi, Erlon . II. Universidade
Federal de Santa Catarina. Programa de Pós-Graduação
em Engenharia Elétrica. III. Título.

Thiago de Alencar Sousa

**HANDLING THE STOCHASTIC HYDROTHERMAL UNIT
COMMITMENT WITH DIFFERENT MODELS OF PIECEWISE
LINEAR HYDROPOWER PRODUCTION FUNCTIONS**

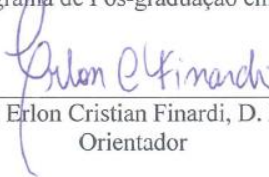
Esta dissertação foi julgada adequada para a obtenção do Título de “Mestre em Engenharia Elétrica”, e aprovada em sua forma final pelo Programa de Pós-graduação em Engenharia Elétrica da Universidade Federal de Santa Catarina.

Florianópolis, 31 de Agosto de 2018.



Prof. Bartolomeu Ferreira Uchôa Filho, Ph.D.

Coordenador do Programa de Pós-graduação em Engenharia Elétrica

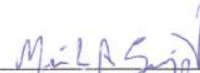


Prof. Erlon Cristian Finardi, D. Eng.
Orientador

Banca examinadora:



Prof.ª Andrea Zanella, Ph.D.



Prof. Murilo Reolon Scuzziato, D. Eng.

À minha mãe, pelo exemplo
de dedicação à família.

AGRADECIMENTOS

Agradeço primeiramente à minha família: *Maria de Fátima*, mãe, *Adriana Macedo*, irmã e *André Macedo*, irmão, pelo imensurável apoio durante este período.

Ao *Prof. Erlon Finardi*, pela orientação do trabalho, diretrizes técnicas, amizade e incentivo em momentos difíceis.

Aos meus amigos *Cairé, Rafael, Cláudio e João Francisco*, os quais eu tive a grande sorte de conhecer em Florianópolis e pude compartilhar grandes momentos da vida durante o mestrado.

Aos meus amigos de Belém, principalmente *Lian e Daniel*, pelos momentos compartilhados não só durante o período do mestrado, mas também em outros momentos prévios da vida que possuem igual importância e sempre serão lembrados como cristas de felicidade ao longo da vida.

Ao meu primo *Daniel* pelos conselhos e compartilhamentos de felicidades e frustrações acerca da trajetória acadêmica.

Aos amigos do PPGEEL, especialmente *Guilherme Fredo, Guilherme Matiussi, Felipe Beltrán, Victor Freitas, Jonas Pesente, Sandy Tondolo e Renata Pedrini*, pelos conhecimentos compartilhados e amizade.

Por fim, agradeço à Coordenação de Aperfeiçoamento de Pessoal de Nível Superior (CAPES), pelo suporte financeiro para a realização do trabalho.

ABSTRACT

The unit commitment (UC) problem seeks to determine which units must operate in a day-head planning horizon. In systems with centralized dispatch and predominance of hydroelectricity, this problem is very complex due to the presence of nonlinearities and a mixed-integer set of decisions. The nonlinearities are associated with the hydro production function (HPF), defined by the product of the net head, turbined outflow, and efficiency of the unit. Moreover, the mixed-integer characteristic is present due to the need of deciding which units must be operating, as well as to represent their specific characteristics of operation such as start-up costs, minimum up/downtime constraints and startups limit. Due to the growing insertion of intermittent sources, e.g. wind farms, it is necessary to consider the inherent uncertainty in this kind of resource, which characterizes the problem as stochastic as well. For large-scale systems, it is not viable to solve this problem with all these characteristics and some simplifications are usually applied to the model. In this work, due to the availability of efficient softwares to solve mixed-integer linear programming (MILP) problems, the nonlinearities of the HPF can be treated with different levels of efficiency. For instance, considering piecewise linear models obtained through the Convex Hull algorithm, it is possible to represent the hydro units individually or through aggregation in one single equivalent generating unit. Each representation has a specific impact in the solution quality and computational effort, which have to be investigated for large-scale problems. In this sense, based on the solution of the deterministic UC instances, we compare three different individual representations of the HPF. Using these results, we define the best representation and compare with the other two ones, which are given by an aggregated representation of the units, through the solution of a two-stage stochastic programming model. Cases involving wind generation scenarios and initial useful volumes of the reservoirs are presented, using the data of a realistic hydrothermal configuration with 11 thermal plants and 16 hydro plants with 52 generating units. In the UC problem, a load is distributed in a transmission system with 95 transmission lines and 46 buses. The planning horizon is one day, discretized in hourly steps. Due to the dimension of the problem, the two-stage model is solved using Benders decomposition, in which the master problem is stabilized with the Proximal Bundle method to improve the convergence of the algorithm.

Keywords: Unit Commitment problem, Hydro Production Function, two-stage stochastic programming, Benders Decomposition.

RESUMO

O problema do comissionamento de unidades geradoras (UGs) visa determinar quais unidades devem operar ao longo do dia seguinte a operação em tempo real. Em sistemas com despacho centralizado e predominância de hidroeletricidade, o problema é muito complexo devido a presença de não linearidades em um conjunto discreto. As não linearidades estão associadas com a função de produção hidrelétrica (FPH), dada pelo produto entre queda, vazão e rendimento da UG. Por sua vez, a característica discreta se deve a necessidade de decidir quais UGs devem estar operando, bem como a representação de características operativas particulares tais como custos de partida, restrições de *minimum up and downtime* e limite no número de partidas das UGs. Com a inserção crescente de fontes intermitentes, e.g. a geração eólica, deve-se levar em conta a incerteza inerente a este tipo de recurso o que, conseqüentemente, caracteriza o problema também como estocástico. Para casos de grande porte, não é viável computacionalmente resolver o problema com todas essas características e comumente algumas simplificações de modelagem devem ser realizadas. Neste trabalho, devido a disponibilidade de pacotes computacionais eficientes de programação linear inteira-mista (PLIM), as não linearidades da FPH podem ser tratadas com diferentes níveis de eficiência. Por exemplo, tendo como base modelos lineares por partes obtidos por *Convex Hull*, pode-se representar as UGs individualmente ou por meio da agregação das mesmas em uma UG equivalente em cada usina hidrelétrica. Cada representação tem um impacto peculiar, em termos de qualidade de solução e esforço computacional, o qual merece ser investigado para casos de grande porte e com predominância de recursos hidrelétricos, como é o caso Brasileiro. Nessa direção, com base na solução de casos determinísticos, comparam-se três maneiras de modelar a FPH por UG. Com base nesses resultados, a melhor estratégia é comparada com duas outras, as quais representam as UGs de forma agregada, por meio da solução de um modelo de programação estocástica de dois estágios. Diversos casos envolvendo cenários de geração eólica e volumes iniciais dos reservatórios são apresentados, tendo como base os dados de uma configuração hidrotérmica realista com 11 unidades termelétricas e 16 usinas hidrelétricas com 52 unidades geradoras. No problema, deve-se atender a uma demanda distribuída em um sistema de transmissão com 95 linhas e 46 barras, ao longo de um horizonte de um dia, discretizado em passos horários. Devido a dimensão do problema, o modelo de dois estágios é resolvido por meio da

decomposição de Benders, no qual o problema mestre é estabilizado com o método de feixes para melhorar a convergência do algoritmo.

Palavras-chave: Problema do comissionamento de unidades geradoras, Função de produção hidrelétrica, programação estocástica de dois estágios, decomposição de Benders.

LIST OF FIGURES

Figure 3-1 - Deterministic cases and characteristics.	50
Figure 4-1 – Scenario Tree.	53
Figure 4-3 - Characteristics of the Stochastic cases.	57
Figure 4-2 - Benders Decomposition.	58
Figure 5-1 - Total load.	70
Figure 5-2 – Hydro plants located in the Iguaçu river.	70
Figure 5-3 - Hydro plants located in the Uruguay River.	70
Figure 5-4 - Power plants, loads, and transmission system configuration.	74
Figure 5-5 – Aggregated wind generation scenarios.	75
Figure 5-6 – Optimal costs for the deterministic MILPs.	77
Figure 5-7 – Computational times (s).	77
Figure 5-8 - Total cost for the 20 Cases.	80
Figure 5-9 - Computational Execution Time (s).	81
Figure 5-10 - Lower and Upper bounds for SF1 case.	83
Figure 5-11 - Lower and upper bounds for SF3 case.	84
Figure 5-12 - Lower and upper bounds for SF1 case (80% vol)	85
Figure 5-13 - Lower and upper bounds for SF3 case (80% vol.).	85
Figure 5-14 – Mean (left axis) and the standard deviation for Tree 1.	86
Figure 5-15 – Mean (left axis) and the standard deviation for Tree 2.	86
Figure 5-16 – Mean (left axis) and the standard deviation for Tree 3.	87
Figure 5-17 - Mean (left axis) and the standard deviation for Tree 4.	87

LIST OF TABLES

Table 2-1 - Main energy sources in the BIS.	29
Table 3-1 - Constraints in the deterministic HTUC models.....	50
Table 3-2 - Variables in the deterministic HTUC models.....	50
Table 5-1 - General data of the hydro plants.....	71
Table 5-2 - Operation zones and productibility.	71
Table 5-3 – HPF data.	72
Table 5-4 - Inflows.	73
Table 5-5 - General data for thermal plants.	73
Table 5-6 - Initial volumes of hydro plants (hm^3).....	76
Table 5-7 – Variables and constraints for individual HPF modeling.	76
Table 5-8 – Average (\bar{x}) and standard deviation (S) of the optimal costs (R\$). ..	78
Table 5-9 - Average and standard deviation of the computational times (s).....	78
Table 5-10 - Turbined outflow in H_5 at stage 6 (m^3/s).....	78
Table 5-11 - Turbined outflow in H_9 at stage 9 (m^3/s).....	79
Table 5-12 - Power generation decisions in H_5 plant in stage 6 (MW).....	79
Table 5-13 - Power generation decisions in H_9 plant in stage 9 (MW).	79
Table 5-14 – Number of variables and constraints for DF4 and DF5 models....	79
Table 5-15 - Average and standard deviation of the optimal costs (R\$).	81
Table 5-16 - Average and standard deviation of the computational time (s).	81
Table 5-17 - Stochastic cases for 10 scenarios.....	82
Table 5-18 - Stochastic cases for model SF1 (40% vol).	88
Table 5-19 - Stochastic cases for model SF3 (40% vol).....	88
Table 5-20 - Stochastic Cases for model SF1 (80% vol).	88
Table 5-21 - Stochastic Cases for model SF3 (80% vol).....	88

LIST OF ABBREVIATIONS AND ACRONYMS

UC	Unit Commitment
ISO	Independent System Operator
PDPM	Programa Diário da Produção em Patamares de 30 minutos
OPCHEND	Operação de Controle de cheias diárias
FCF	Future Cost Function
HPF	Hydro Power Function
ONS	Operador Nacional do Sistema
MILP	Mixed-Integer Linear Programming
BD	Benders Decomposition
BB	Branch and Bound
MIP	Mixed Integer Programming
RO	Robust Optimization
CCO	Chance-Constrained Optimization
SO	Stochastic Optimization
LP	Linear programming
HTUC	Hydrothermal Unit Commitment
BIS	Brazilian interconnected system
SDDP	Stochastic Dual Dynamic Programming
GHG	Greenhouse gas
MTGS	Mid-term generation scheduling
STGS	Short-term generation scheduling
DE	Deterministic Equivalent
PDF	Probability Density Functions
MRE	Mean Relative Error

CONTENTS

1. Introduction	21
1.1 Relation with Existing Literature	22
1.2 Goals of the Thesis	27
1.3 Outline of the Thesis	27
2. The Brazilian Generation Scheduling Problem.....	29
2.1 Penetration of Renewable Energy	31
2.2 Generation Scheduling Problems	32
3. Deterministic Unit Commitment Model.....	35
3.1 Thermal Plants.....	35
3.2 Transmission System.....	37
3.3 Hydropower plants	38
3.3.1 Nonlinear Hydro Power Function	41
3.3.2 Individual Model (DF1)	42
3.3.3 Individual Model with Equal Generation (DF2)	44
3.3.4 Individual Model with Aggregated Constraints (DF3)	44
3.3.5 Aggregated Units with one Binary Variable per Plant (DF4)	46
3.3.6 Aggregated Units without Binary Variable (DF5).....	47
3.4 Hydrothermal Unit Commitment Model	48
4. The Hydrothermal Unit Commitment Problem via Two-Stage Stochastic Programming	51
4.1 Methods for Optimization under Uncertainty.....	51
4.2 Multi-stage Stochastic Optimization	52
4.3 Two-stage Stochastic Optimization.....	53
4.3.1 Stochastic model 1 – SF1	54
4.3.2 Stochastic Model – SF2.....	56
4.3.3 Stochastic Model – SF3.....	56
4.4 Benders Decomposition.....	57
4.4.1 BD Algorithm	58

4.4.2 Optimality cut	60
4.5 Stabilized BD via Proximal Bundle Method	66
5. Computational Results	69
5.1 Electrical System.....	69
5.1.1 Hydro Plants	70
5.1.2 Thermal Plants	73
5.1.3 Transmission System	73
5.1.4 Wind Power Scenario Generation	74
5.2 Deterministic cases.....	75
5.2.1 Individual Representation of the Hydro Units	76
5.2.2 Aggregated Hydro Units	79
5.3 Stochastic Instances	81
5.3.1 Reservoirs with 40% Initial Volumes	82
5.3.2 Reservoirs with 80% Initial Volumes	84
5.3.3 Additional Computational Instances	85
6. Concluding Remarks	91
6.1 Suggestions for future works.....	92
7. Appendix a: Transmission Lines Capacity	93
8. References	95

1. INTRODUCTION

The Unit Commitment (UC) problem in electric power systems planning might be defined as finding a schedule that defines which generation units must be turned on/off throughout a specified planning horizon. This schedule needs to satisfy the constraints of the system such as energy load requirements, generation limits of the units, transmission lines capacity, etc. Furthermore, this schedule is also defined so that an objective function must be minimized over that planning horizon. In electricity markets with centralized dispatch approach, since an Independent System Operator (ISO) is responsible for ensuring the social and economic welfare of the market, the objective function is usually given by the expected cost associated with thermal generation and deficit. On the other hand, in a decentralized approach, the generation companies supply bids with price and quantity for selling energy and thus the objective function is composed of the net revenues. Thus, independent of the market regulation framework, the UC problem is a well-known (and hard-to-solve) optimization problem.

In the case of this work, the interest is the centralized dispatch approach where the generating units of the system are given by hydro, thermal and wind resources. The power generated by wind farms are considered uncertain. Even though the UC has been studied by many researchers in the last decades, this is not a well-solved problem, mainly when we regard large-scale systems with predominance of the hydro resources.

The presence of hydro plants inserts reasonable difficulties in this optimization problem. In many systems, mainly the ones with several hydro units, some plants may be coupled in cascade, which means that the reservoir water level of a downstream plant is influenced by the generation of the upstream plant. Besides that, the generation cost for hydro plants is not measured in the same way as for thermal plants, i.e., based on the amount of fuel used in the start-up, shutdown and nominal operation procedures. One methodology to measure the water cost is the Future Cost Function (FCF) (PEREIRA, 1989), which is represented by a set of inequalities constraints and it is included as a boundary condition for the UC problem. Moreover, forbidden zones associated with the Hydro Power Function (HPF) also may add difficulties to solve the problem. The HPF is a nonlinear and nonconvex function that is, in general, linearized for practical purposes; thus, the UC problem can be handled with mixed-integer linear programming (MILP) solvers. This

linearization, depending on the method used and the accuracy level, may result in many constraints and variables. All these issues affect directly the convergence of the UC problem even in the deterministic setting.

As it is known, the recent growth in the use of renewable energy sources, mainly wind generation, inserts uncertainty in the UC problem so that in certain cases the computational burden may become infeasible. Therefore, new techniques and models have been proposed to overcome these issues related to the UC problem with a predominance of hydro resources. In this scenario, the focus of this work consists in evaluating a tradeoff between computational burden and accuracy related to the hydro plant model in the UC problem. The main goal is to explore different representations of the HPF, considering aggregated and individual units when the UC is represented as a two-stage stochastic programming model. The scenario tree is associated with the wind generation and the resulting optimization model is solved via Benders decomposition (BD)-based techniques.

1.1 Relation with Existing Literature

The first studies related to the UC problem were performed during the 1960s for thermal systems. Since that time, many researchers have been working on this subject, which became known as thermal UC problem (WRIGHT & JOHNSON, 1971), (HARA, et al., 1966) (PANG & CHEN, 1976), (COHEN & YOSHIMURA, 1983). Due to the mixed-integer nature, and also the complexity of the problem, especially when applied to large-scale power systems, different optimization approaches have been applied over the past years, such as priority ordering methods (LEE, 1988), dynamic programming (SNYDER, et al., 1987), (BOSCH, 1985), Lagrangian relaxation (MUKHERJEE & ADRIAN, 1989), (PETERSON & BRAMMER, 1995), Benders decomposition (SHAHIDEPOUR, et al., 1997), branch-and-bound method (COHEN & YOSHIMURA, 1983) and mixed-integer linear programming (CHANG & WAIGHT, 1999), (MUCKSTADT & WILSON, 1968). Most of these first works considered the UC as a deterministic problem; however, with the advent of renewable energy sources and computers with more data processing capacity, it was possible and necessary to consider the UC problem in a stochastic setting.

Starting with determinist UC approaches, priority order is usually the simplest among the mentioned methods. In such approach, the units are committed to ascending order of their average production cost (GOVARDHAN, 2016), i.e., units are committed in a fixed order until

the commitment of the next unit in the priority list is uneconomic or more expensive. Nevertheless, priority list methods often result in sub-optimal solutions, even in deterministic UC problems, since it usually does not handle difficult constraints (KAUR BAWA & KAUR, 2013). Nowadays, in some specific works, priority methods are usually combined with other methods such as dynamic programming or meta-heuristics to solve UC problems under uncertainty.

Dynamic programming (DP) is one of the most classical approaches to solving UC problems. This method evaluates many decisions associated with the state space in a multi-stage problem. A subset of decisions is associated with each sequential stage problem and the cheapest one must be selected to minimize costs, i.e., a single decision must be made in each problem step. There is a cost associated with each decision and this cost may be affected by the decision made in the preceding step. This algorithm evaluates systematically many possible decisions in terms of minimizing the overall cost in a multistage scheduling problem (OUYANG & SHAHIDEPOUR, 1991). Due to the enumerative nature of the method, DP suffers from a long processing time that expands exponentially with the size of the problem. The use of this method nowadays involves mostly solving subproblems of UC often in relation with Lagrangian-based decomposition methods (TAHANAN, et al., 2018).

Lagrangian relaxation (LR) is included in the “dual decomposition” methods. This approach decomposes the original primal problem into smaller easy-to-solve subproblems. For obtaining the decomposition, using Lagrange multipliers, the LR relaxes the coupling constraints, such as demand and reserve requirement ones, by moving them into the objective function. This method has the advantage of being easily modified to model characteristics of specific utilities and is robust in handling several types of the unit constraints. On the other hand, its optimal solution rarely satisfies the relaxed constraints. Besides that, the method is sensitive which may cause unnecessary commitments of some units so that depending on the specific problem only a suboptimal feasible solution can be expected from the LR (SALAM, 2007). However, the LR is still one of the most used methods, mainly in optimization under uncertainty due to the computation time when compared to other mathematical approaches.

Another classical approach to solve UC problems is the Benders Decomposition (BD), which is a primal decomposition. The BD decomposes the original problem into one master problem and other smaller subproblems. The master problem carries the fixed “complicated” variables (usually binary ones), and the subproblems have, in general, the

“easy” ones (continuous), thus easier independent problems to solve (BONNANS, et al., 2006). The application of BD to the UC problem is also seen in this work and therefore it will be better discussed in Chapter 4.

Branch and bound (BB) is a technique that solves simpler problems derived from a more complex original problem. These less complicated problems compose a tree, and each problem solution gives a lower bound on the solutions of the problems that are descendants of that one. However, if the cost solution of a problem is greater than a feasible solution to the original problem, then it is not necessary to evaluate the nodes below derived from that one since there will not be the optimal node among them (COHEN & YOSHIMURA, 1983). The great disadvantage of the BB method is that execution time grows up exponentially with the size of the UC problem. Besides that, using approximations for making the problem tractable for large-scale systems causes solutions to be highly sub-optimal (CHENG, et al., 2000).

Mixed-integer programming (MIP) techniques consist of implementing mixed-integer models using qualified software to solve these sorts of problems. MIP formulations of UC have become common with the rise of data processing and efficiency of mixed-integer linear programming (MILP) solvers, such as GUROBI and CPLEX. Nowadays, MILP techniques are universally used when combined with other approaches, such as LR, DP, etc. Nevertheless, depending on how detailed the model is, MILP techniques might demand much computational effort. As detailed ahead, the MILP technique is used in this work to perform some deterministic analysis of the UC problem.

All the methods mentioned to handle the deterministic UC are also used in the stochastic UC problems. In general terms, MILP, LR, BD, DP, etc., are (alone or combined) the core solution strategy in the following approaches: Robust Optimization (RO), Chance-Constrained Optimization (CCO) and Stochastic Optimization (SO) (also known as a scenario-based approach). The basic ideas of these methods will be better explained in chapter 4, but by now the main works that approach these methods are discussed.

In general, the UC under uncertainty uses probability (scenario or distributions) associated mostly to four aspects in the problem: availability of the units, load, wind, and inflow (CARDOZO, 2014). Energy prices may be present in the models, especially in decentralized market framework approaches. For example, Jiang, et al. (2010) use a two-stage model to treat uncertainty on supply and demand. Uncertain problem parameters are assumed to be within a given cardinality or polyhedral

uncertainty set. Conclusive results compare the RO technique with a deterministic approach.

The CCO was first applied in the UC problem by Ozturk et al. (2004). In this work, LR was used to decompose the original primal problem into subproblems and each one was solved by DP. Moreover, the Monte Carlo method is used to verify the accuracy provided by the CCO technique. Ding, et al. (2010) propose a technique using CCO in where probabilistic constraints are changed into deterministic ones, and then a simple MILP method is used to solve the problem completely. The authors consider uncertainty on demand fluctuations, unit forced outages, a variety of energy prices and wind generation.

The SO approach has been used broadly in the UC context over the past few years. An early work is presented by Carpentier et al. (1996). Random disturbances are modeled as scenario trees and the technique optimizes the average generation cost of the tree. To solve the problem, an augmented Lagrangian technique is used. Wong and Fuller (2007) present a stochastic linear programming (LP) formulation using scenario trees to model uncertainty associated with energy prices. The authors use an LP technique to solve the problem since simplifications were performed in the mathematical model with the goal to focus on energy prices stochastic schemes. The SO approach is also the method to represent uncertainty in this work to solve the UC problem.

Another critical issue related to any UC problem is the mathematical model associated with the elements of the system. The more details and variables in the model, the harder it is to find an optimal solution. Researchers have been inspecting many different models since the UC problem begun being studied. Considering the Hydrothermal UC (HTUC) problem, some detailed models can be seen in works such as of Takigawa (2010), Tavlaridis-Gyparakis (2017), Liahagen and ROD (2016), Gil et al (2003), Paredes et al (2015), Martins and Soares (2014), Norbiato, et al (2014).

In the HTUC associated with hydro-based systems, one of the crucial aspects associated with the mathematical model is the accurate modeling of the HPF (CHENG, et al., 2000), which is a nonlinear function of the net head, turbined outflow and global efficiency of the unit. Thus, due to its nonlinear nature and nonconvexity, the precise inclusion of this function in the problem is a challenging task. There must be a balance in the model neither to oversimplify the model and find infeasible solutions for real-time operations, nor to implement many details that may result in impractical computation times.

In Carvalho (2002) the HPF considers individual units. The hydro generation is obtained through a linear relationship between power and turbined outflow. The linear coefficient that links these two variables is the productivity ($\text{MW}/(\text{m}^3/\text{s})$), which is a constant value calculated using the forebay, tailrace, and losses for discretized values of useful volume. This representation may be used for preliminary studies in the UC, but is more often used on the medium-term planning, since it is also considered simplified for the short-term. In Cunha et al. (1997), the authors present a method to calculate a variable productivity based on the concept of energy production function. The method assumes that the total production of energy is obtained from volume values, turbined outflow, and spillage. This is a more realistic approach and it has been used in the entire Brazilian system to optimize the operation planning in the medium-term. In Conejo *et al.* (2002) a MILP model is proposed to compute the power generation considering the net head and water discharged for each hydro unit. Regarding the HPF, the authors simplify the Hill chart using unit performance curves for specified values of the head. Furthermore, these curves consist of piecewise linear functions selected by binary variables. In this sense, this model has as disadvantage the excessive use of binaries. The methodology presented by Diniz and Maceira (2008) uses the concept of Convex Hull (CH) (ANDREW, 1979), which is a strategy to sketch plans that envelops the original function throughout its domain. The model considers the influence of the stored volume, turbined outflow, and spillage in the HPF. On the other hand, the efficiency of the units is considered constant and hydraulic losses are calculated as percentages (or fixed values) of the gross head. In Li *et al.* (2014) a case study of hydro UC for the Three Gorges Project, in China, is presented. Concerning the HPF, the model considers the head variation over the operation and its effects on power generation. The forebay level is formulated using a linear approximation, but for the tailrace, an ad-hoc procedure is used using sequential MILP executions until achieving convergence. Moreover, the penstock head loss function is considered constant. The work of Guedes *et al.* (2017) proposes a compact MILP formulation based on an equivalent unit model and a piecewise linear generation function, which provides an aggregated optimal solution that is used to obtain unit decisions.

1.2 Goals of the Thesis

This work seeks to evaluate the impact of different piecewise linear models of the HPF on the stochastic HTUC problem. The main goal is to investigate the tradeoff between computational burden and solution quality in the HTUC when different HPF representations are included in this problem. In general terms, two types of HPF models are analyzed: a single continuous function that aggregates the identical units in the plant, and the classical discontinuous HPF individual representation that considers each unit separately. As detailed ahead, we present three possibilities for representing the individual HPF and, for accessing the best approach, we perform a comparative analysis of these ones via deterministic HTUC problem. In the sequence, we use the individual model chosen in the deterministic setting to compare with the aggregated model in a two-stage stochastic HTUC problem.

1.3 Outline of the Thesis

The thesis is structured as follows: Chapter 2 briefly describes the context of the generation scheduling planning problem considering the Brazilian system; Chapter 3 presents the mathematical models for each element of the system (generating units, transmission lines, etc.). Besides that, different formulations for the HPF are shown, which define distinct models that will be evaluated in this work. Afterward, the deterministic model for the HTUC problem is presented as a MILP problem; in Chapter 4, initially, the two-stage model is presented. After that, the decomposition method is described, which includes the BD and the Proximal Bundle algorithms; Chapter 5 presents the computational results carried out for the deterministic and stochastic instances, evaluating the different cases defined by each different HPF model; finally, in Chapter 6, the final conclusions are presented, as well as suggestions for further works.

2. THE BRAZILIAN GENERATION SCHEDULING PROBLEM

The Brazilian interconnected system (BIS) is responsible for generation, transmission, and distribution of electric energy throughout Brazil. The system encompasses more than 99% of the Brazilian territory, and only a few small systems (located in the Amazon region) are operated in the island mode (BRITO, 2013). The BIS has also a great extension when compared to other electric power systems abroad, which makes the system unique and extremely hard to operate, especially due to the weak electrical connection with other systems. Regarding power generation, BIS has as its main source the hydropower plants, which has approximately 65% of the total installed power, followed by other secondary sources, such as thermal and wind, as shown in Table 2-1.

Table 2-1 - Main energy sources in the BIS.

Type	Units	Installed power (MW)	(%)
hydro	1,267	98,814	64.55
wind	461	11,245	7.30
solar	55	236	0.15
thermal	2,928	41,101	26.70
nuclear	2	1,990	1.29

Source: modified from ANEEL(2017)

The centralized operation of the BIS is performed by an Independent System Operator (ISO), which has the following obligatory tasks (ONS, 2017):

- 1. Transmission system reinforcement:** ISO elaborates a study called Enlargement and Reinforcement Plan, whose objective is to determine the changes in the transmission network, besides the reinforcement on the equipment of transmission and distribution companies;
- 2. Integration of new systems:** The Brazilian regulatory framework assures that any agent can be connected to the transmission system if the new integration has the requisites and criteria established by the ISO;
- 3. Mid and Short-term generation scheduling:** ISO evaluates future conditions to provide enough energy so that a certain demand is supplied. In the mid-term scheduling, the planning

horizon is 5-years discretized monthly steps. The hydro resources are modeled based on the concept of “equivalent subsystems”. On the other hand, the short-term scheduling has a two-month planning horizon discretized in weekly steps in the first month. This problem uses the FCF calculated by the mid-term scheduling and the hydro resources are represented in an individualized way. Both planning problems are solved using SDDP related algorithms to optimize costs and guarantee the security operation of the system;

4. **Unit commitment (or day-ahead generation scheduling):** it concerns with day-ahead evaluation of the energy supplying conditions, considering a detailed model for the generating units and the transmission system. It defines the commitment and dispatch for hydro, thermal and wind units. Besides that, this stage also decides energy exchange between subsystems and agents of the BIS, as well as energy trade between international connections to supply the load that was previously forecasted;
5. **Real-time operation:** it may be divided into three tasks. The first one tries to apply the decisions coming from the day-ahead, with changes when necessary. The second one coordinates and supervises the network and its functioning, acting when some contingency or another event unexpected happens. The last one checks the data to evaluate the occurrences of the other stages, analyzing perturbations and contingencies;
6. **Evaluation of the operation:** identifies undesirable causes and events related to unsatisfying performances of the system, and elaborates recommendations to improve the operation;
7. **Managing of transmission:** it produces information that will compose the payments for those who provide the transmission lines services.

Due to the size and the changes that the system has been going through, such as new environmental politics and penetration of renewable sources, there is a need of novel studies to contribute for a high-quality operation. The next section will point out a few of these changes.

2.1 Penetration of Renewable Energy

There is a growing use of renewable energy sources in power systems throughout the world, due to the advantages related to environmental politics, since renewable sources usually have minor impacts, reduced operating costs and do not depend on oil price variations. Wind power has not been used in large scale until the 1990s. By 1997, 1.5 GW of new capacity was installed worldwide (7.6 GW total global capacity), and it kept growing until 2013 when it suffered a dramatic decline in new installations. However, this growth was quickly recovered and in 2015 wind power reached 432.9 GW, which stands for a 5,596% growth in 20 years (GWEC, 2015). Photovoltaic energy has followed the same path, but its use in large-scale started only during the 2000s. In 2008, the global capacity was 16 GW, and in 2015 it summed up 230 GW around the globe, a 1,331% growth in 10 years.

Energy generation in Brazil followed a similar behavior, being among the top countries whose wind power capacity had the biggest growth in 2015 (46.2%). Nowadays wind energy sums up an expressive amount of generation among the main energy sources in Brazil. Solar energy is not as used as wind, but it is also increasing, and Brazil is supposed to be among the 20 top countries with the greatest generation of solar energy in 2018 (PORTAL BRASIL, 2016).

Brazil stands out for having an energy matrix with a substantial share of renewables. Besides the increase in solar and wind energy, the main energy source in Brazil is also renewable, coming from several hydropower plants, a reality observed in a few countries in the world. This means that, currently, the GHG (greenhouse gas) emissions per unit of energy consumed in Brazil are far below when compared to other countries. On the other hand, if we compare socioeconomic indicators, we realize that Brazil still has a long way to go to reach a human development index comparable to those of developed countries. Hence, even though Brazil has been adopting a development path less intensive in energy use than other nations, it is hard to imagine that the nation will be able to reduce the poverty level on the horizon by 2030 without increasing energy consumption, since both are connected. As a result, GHG emissions will rise. Thus, the great defy of the Brazilian energy sector is precisely to keep a high share of renewable sources in its energetic matrix, which implies a significant expansion of the existing number of wind farms, solar plants, biomass-fueled thermal power plants and the construction of new hydroelectric plants, in addition to increas-

ing production and consumption of liquid biofuels, ethanol and biodiesel, and investments in energy efficiency (EPE, 2016).

Nowadays, most of the hydroelectric inventoried potential is in the Amazon and Tocantins-Araguaia river basins, where there are large extensions of protected areas (conservation units, indigenous lands, and lands occupied by staying “quilombo” communities). Due to this social and environmental context, hydroelectricity is expected to lose share in the following years, at the expense of an increased share of wind, solar and biomass sources. Even though renewable sources have many advantages, they also have disadvantages, which include prohibitive costs to build a facility, dependence on geographic conditions (such as hydropower plants that depend on rivers flow) and intermittency of energy supplying. This last one is what makes a large system as BIS hard to operate with high penetration of renewable sources, since some forecasts might be hard to obtain, such as wind speed and inflows.

Hydropower plants with reservoirs provide more reliability concerning energy supplying, but nowadays many facilities without a reservoir, i.e., run-of-the-river plants, are being built and operated in the world, mainly due to environmental politics since there are major impacts related to the construction of reservoirs. Thus, considering the Brazilian context, due to the presence of hydro plants with large reservoirs and the absence of wind farms in the past, there was a tendency to develop mathematical models concerning only medium and long terms. However, nowadays with this change in the Brazilian scenario towards renewable energy, run-of-the-river plants, and wind farms, new challenges are emerging and then we need to develop a substantial stochastic UC model.

2.2 Generation Scheduling Problems

The complexity of BIS makes infeasible to solve a unique computational model to accomplish the generation scheduling problem. Thus, ISO works with three main computational models, each one possessing different detail levels in the modeling (uncertainties, nonlinearities, on-off decisions). The computational models are associated with the following operational tasks: Mid-term generation scheduling (MTGS), short-term generation scheduling (STGS) and the UC problem.

MTGS problem is solved annually and revised every four months. This problem has as the main goal to evaluate the energy supplying to the forecasted energy market for a 5-years planning horizon, giving relevant information to the expansion of the system (ONS, 2017). The

main computational tool used to perform these evaluations is the NEWAVE model (DINIZ & MACEIRA, 2008), which defines via Stochastic Dynamic Dual Programming (SDDP) the water values for energy equivalent model in each month.

Using the water values provided by MTGS, the STGS problem is solved monthly and revised every week. The two-months planning horizon is discretized weekly according to the load level in the first month, and the inflows in the second monthly are considered random. The main tool responsible for this study is the computational model DECOMP, in which each hydro plant is represented through its physical characteristics and operational constraints. The DECOMP model employs the L-Shaped algorithm as the solution strategy and, as a result, at the end of the first week, the water values are available as a function of the storage and past inflows. The last step of generation scheduling in Brazil is the so-called UC problem.

The UC has as its main goal to optimize the operation of BIS, supplying energy to the demand with security and on the best technical conditions. To carry out this goal, the HTUC performed by ONS uses as input data: centralized load forecasts performed every 30 minutes, daily meteorological data to forecast the wind conditions, availability declarations of power plants and forecasted inflows. It is also considered environmental constraints, maintenance schedules of generation and transmission installations, and operational constraints of the power plants. All this information, together with the generation dispatch, power exchanges between subsystems and daily load programs compose the final report of the day-ahead generation scheduling, aggregating its input information and outcomes discretized in 30 minutes for the entire day.

The computational tools used in this step are PDPM and OPCHEND (ONS, 2016). The first one works on the managing and validation of the other models acting on the previous steps, verifying the energetic balance, exchanges, reserve generation and thermal generation. The second one concerns goals related to the levels of the reservoirs that were established by preceding steps (ONS, 2008).

This work treats the UC problem, analyzing it from a mathematical perspective. Thus, it is a problem that has a substantial mathematical complexity which can be summarized in TAKIGAWA (2010):

- time coupling: due to the storage limits, water time traveling, ramp and uptime and downtime of thermal generation;
- space coupling: due to hydro plants in cascade, power flow equations;

- nonlinear: because of the HPF, operational costs of thermal units and power flow between transmission lines;
- combinatorial: since one of the main goals of the operation programming is to decide which units should be on or off to supply enough energy to meet the demand;
- size of the system: due to the substantial number of the units, time stages, binary decisions, and uncertainties.

Thus, the nature of the HTUC is a mixed integer nonlinear optimization problem. Some features of this nature might be loosed, such as non-linearity, changing, for instance, the hydroelectric production function and the power flow in transmission lines to linear approximations, which improves the computational effort to solve the problem. The assumptions made in this thesis regarding the HTUC problem will be better explained in the next chapter.

3. DETERMINISTIC UNIT COMMITMENT MODEL

This chapter presents the deterministic optimization model used in this work to handle the HTUC problem. Initially, costs and constraints of thermal plants are introduced. After that, the DC power flow model is presented. Next, the model for the hydro generating units is shown, which includes different approaches of the HPF. Finally, the entire mathematical model is presented as a deterministic MILP problem.

3.1 Thermal Plants

Thermal plants use the energy of heat to generate electricity. The fuel used in this process can be a fossil, nuclear or renewable. In usual thermal plants, the procedure of burning this fuel produces the heat that turns water into steam, which will drive the inner turbine producing kinetic energy. The generator produces electricity from the turbine movement. This energy production involves a cost, which can be divided into start-up and nominal operation costs. The latter is usually modeled by a first or second-order (convex) polynomial that depends on the power output of the generating unit. Since second-order polynomials might increase computational effort to solve MILP problems, in this work is used one first-order polynomial, as the following equation:

$$oc_{it} = \mathbf{C}_i \cdot pt_{it} + \mathbf{FC}_i, \quad (3.1)$$

where:

- oc_{it} variable thermal cost of plant i and stage t when the unit is operating in nominal range (R\$);
- \mathbf{C}_i unitary variable cost of plant i (R\$/MW);
- pt_{it} generation of thermal plant i and stage t (MW);
- \mathbf{FC}_i the fixed cost of thermal plant i (R\$).

Besides oc_{it} , the act of turning on a thermal plant yields a cost since there is a time interval until the plant starts producing its minimum power. Then, considering as a fixed value, the fuel used during this time can be modeled through a start-up cost (WOOD & WOLLENBERG, 1996) as detailed in (3.2).

$$\begin{aligned} sc_{it} &\geq (u_{it} - u_{i,t-1}) \cdot \mathbf{SC}_i, \\ sc_{it} &\geq 0, \end{aligned} \quad (3.2)$$

where:

- sc_{it} auxiliary continuous variable to compute the start-up cost of thermal i and stage t (R\$);
- \mathbf{SC}_i the start-up cost of thermal plant i (R\$);
- u_{it} binary variable that indicates if thermal plant i is on ($u_{it} = 1$) or off ($u_{it} = 0$) in stage t .

The power produced by a thermal plant does not change loosely along a time horizon. Then, constraints known as ramp prevent this power variation to be higher than a determined value, and this variation must be limited in situations when power is decreasing or increasing. Equations (3.3) and (3.4) represent ramp constraints (FRANGIONI, et al., 2009). The first one corresponds to the situation when generated thermal power is increasing, and the second one to power decreasing.

$$pt_{it} \leq pt_{i,t-1} + u_{i,t-1} \mathbf{R}_i^{up} + (1 - u_{i,t-1}) \mathbf{PT}_i^{\min}, \quad (3.3)$$

$$pt_{i,t-1} \leq pt_{it} + u_{it} \mathbf{R}_i^{down} + (1 - u_{it}) \mathbf{PT}_i^{\min}, \quad (3.4)$$

where:

- $\mathbf{R}_i^{up(down)}$ ramp-up (down) rate limit of thermal plant i (MWh/h);
- \mathbf{PT}_i^{\min} minimum power of thermal plant i (MWh).

The equations above limit the ramp rate when a plant is already online, but also when a unit is turned on/off. In this case, it is mandatory to generate minimum power in the previous stage before the unit turns on or shuts down.

Other important operational characteristics are given by the minimum up and downtime constraints, which avoid the mechanical stress of thermal plants ensuring that a plant will be on/off for a minimum time interval. These constraints are formulated by equations (3.5) (FRANGIONI, et al., 2009).

$$\begin{aligned} u_{it} &\geq u_{ic} - u_{i,c-1}, c \in [t - \mathbf{TT}_i^{up} + 1, t - 1], \\ u_{it} &\leq 1 + u_{ic} - u_{i,c-1}, c \in [t - \mathbf{TT}_i^{down} + 1, t - 1], \end{aligned} \quad (3.5)$$

where:

- $\mathbf{TT}_i^{up(down)}$ minimum uptime (downtime) of thermal plant i after turning on/off the plant. (h).

Due to thermodynamic and efficiency issues, thermal plants have minimum and maximum power values, according to (3.6).

$$\mathbf{PT}_i^{\min} u_{it} \leq pt_{it} \leq \mathbf{PT}_i^{\max} u_{it}, \quad (3.6)$$

where:

$\mathbf{PT}_i^{\max(\min)}$ maximum (minimum) power of thermal plant i (MW).

3.2 Transmission System

The transmission system is an important modeling issue since primal decisions may change according to the power flows on the transmission lines. Originally, power flow equations have a non-linear nature, but this aspect is simplified in this work due to the computational effort, and then a classical DC model is used. In this sense, some factors must be considered:

- All bus voltages are considered fixed and equal to 1 p.u.;
- Only the reactance of the transmission lines is considered. Resistances and admittances are negligible;
- Angle (Θ) differences between buses are small, so that $\sin(\Theta) \approx \Theta$ radians.

Thus, with these considerations, it is possible to model power flow in each transmission line via linear constraints, as seen in equations below (TSENG, 1999).

$$-\mathbf{FL}_l^{\max} \leq \sum_{b=1}^{\mathbf{B}} \Gamma_{lb} \left(\sum_{r \in \mathbf{R}_b} ph_{rt} + \sum_{i \in \mathbf{I}_b} pt_{it} + \sum_{g \in \mathbf{RW}_b} \mathbf{PW}_{gt} + pd_{bt} - \mathbf{L}_{bt} \right) \leq \mathbf{FL}_l^{\max} \quad (3.7)$$

On the other hand, the equation (3.8) shows the power balance constraint for the entire system.

$$\sum_{b=1}^{\mathbf{B}} \sum_{r \in \mathbf{R}_b} ph_{rt} + \sum_{b=1}^{\mathbf{B}} \sum_{i \in \mathbf{I}_b} pt_{it} + \sum_{b=1}^{\mathbf{B}} \sum_{g \in \mathbf{RW}_b} \mathbf{PW}_{gt} + \sum_{b=1}^{\mathbf{B}} pd_{bt} = \sum_{b=1}^{\mathbf{B}} \mathbf{L}_{bt} \quad (3.8)$$

where:

- \mathbf{B} number of buses;
- \mathbf{R}_b set of indices of the hydro plants connected to bus b ;
- \mathbf{RW}_b Set of indices of the wind farms connected to bus b ;
- \mathbf{I}_b set of indices of the thermal plants connected to bus b ;
- \mathbf{FL}_l^{\max} maximum power flow capacity of the transmission line l (MW);
- Γ_{lb} power transfer distribution factor (PTDF) of transmission line l due to the injection of active power at bus b ;

- pd_{bt} the deficit of bus b and stage t (MW);
- \mathbf{L}_{bt} load demand of bus b and stage t (MW);
- ph_{rt} power of hydro plant r and stage t (MW);
- \mathbf{PW}_{gt} wind power of wind farm g and stage t (MW).

Above, Γ_{lb} is a dimensionless parameter that depends on the reactance of the transmission lines and represents the sensitivity of each power injection at bus b over line l . Furthermore, Γ_{lb} is obtained through manipulations on equations of power flow, power balance on buses and incidence matrix (SCUZZIATO, 2016). The value Γ_{lb} is zero for the slack bus, i.e., a power injection at this bus has no influence on the other buses. The reference VAN DEN BERGH, et al. (2014) adds more details on how to calculate parameter Γ_{lb} . This DC formulation is helpful if bus angles are not needed since it decreases the number of power flow constraints as well as the number of variables.

3.3 Hydropower plants

Two types of hydropower plants are considered in this work: run-of-the-river and accumulation power plants. There is also a third type of plant with storage by pumping, but this one is not usual on the Brazilian system (SCUZZIATO, 2016) and then it is not considered in this work. Run-of-the-river plants have a small capacity of water storage so that the stored water needs to be used on a short-term period. In turn, hydro accumulation power plants have reservoirs capable of storing water to use during longer time horizons.

The generation cost for hydro plants cannot be computed such as for thermal plants, which is based on the fuel, start-up, maintenance cost and etc. One methodology to measure the water cost is the Future Cost Function (FCF) (PEREIRA, 1989). This function relates the expected cost at the end of the UC planning horizon with the reservoirs storage levels. The more water is stored in the reservoirs, the less expensive will be the expected future costs. Thus, it is possible, using the FCF, to compare costs regarding how much water should be used with keeping the water stored during the UC horizon, considering that it may be operated as an alternative option in the presence of a more expensive source of energy. The equation (3.9) shows the FCF constraints.

$$\alpha + \sum_{r=1}^{n_r} \pi_r^{(g)} v_{r,T} \geq \Lambda^{(g)} \quad (3.9)$$

where:

α	variable that represents the expected future cost (R\$);
$\pi_r^{(g)}$	slope coefficients of the FCF of hydro plant r and cut g (R\$/hm ³);
v_{rT}	volume of reservoir r in the time stage T (hm ³);
$\Lambda^{(g)}$	linear coefficient of the cut g (R\$).

Hydropower units also have some operational characteristics that restrict their operation concerning the range of power generation. Besides that, hydropower plants have a minimum and maximum capacity of stored volume. Thus, constraints (3.10) represent limits of power generation, turbined outflow in the generating units, reservoir volume, and spillage.

$$\begin{aligned}
 z_{jrt} \mathbf{Q}_{jr}^{\min} &\leq q_{jrt} \leq \mathbf{Q}_{jr}^{\max} z_{jrt} \\
 z_{jrt} \mathbf{PH}_{jr}^{\min} &\leq ph_{jrt} \leq \mathbf{PH}_{jr}^{\max} z_{jrt} \\
 \mathbf{V}_r^{\min} &\leq v_{rt} \leq \mathbf{V}_r^{\max} \\
 s_{rt} &\leq \mathbf{S}_r^{\max}
 \end{aligned} \tag{3.10}$$

where:

q_{jrt}	turbined outflow of hydro unit j , plant r and stage t (m ³ /s);
$\mathbf{Q}_{jr}^{\max(\min)}$	maximum (minimum) turbined outflow of hydro unit j and plant r (m ³ /s);
ph_{jrt}	generated power of hydro unit j , plant r and stage t (m ³ /s);
$\mathbf{PH}_{jr}^{\max(\min)}$	maximum (minimum) power generation of hydro unit j and plant r (m ³ /s);
z_{jrt}	binary variable that indicates if hydro unit j , plant r and stage t is on (1) or off (0);
v_{rt}	reservoir volume of hydro plant r and stage t (hm ³);
$\mathbf{V}_r^{\max(\min)}$	maximum (minimum) reservoir volume of hydro plant r (hm ³);
s_{rt}	spillage of hydro plant r and stage t (m ³ /s);
\mathbf{S}_r^{\max}	maximum spillage of hydro plant r (m ³ /s);

Regarding the reservoirs, the operation of hydropower plants is ruled by the principle of mass conservation applied to fluids, which is presented in the equation (3.11).

$$v_{rt} - v_{r,t-1} + \mathbf{C}_1 \left[w_{rt} + s_{rt} - \sum_{m \in \mathfrak{R}_r^{up}} (w_{m,t-\Omega_{mr}} + s_{m,t-\Omega_{mr}}) - \mathbf{Y}_{rt} \right] = 0 \quad (3.11)$$

where:

- \mathbf{C}_1 constant used to convert a turbined outflow (m³/s) into a stored volume (hm³) for a period of 1 hour;
- w_{rt} turbined outflow of hydro plant r and stage t (m³/s), which is given by $w_{rt} = \sum_{j=1}^{NG_r} q_{jrt}$;
- \mathfrak{R}_r^{up} set of indexes of the hydro plants upstream of plant r ;
- Ω_{mr} water traveling time between reservoirs m and r (h);
- \mathbf{Y}_{rt} incremental inflow in the reservoir r and stage t (m³/s).

Likewise thermal plants, hydro units also have minimum up and downtime constraints, expressed in (3.12) as follows:

$$\begin{aligned} z_{jrt} &\geq z_{jrc} - z_{jr,c-1}, c \in [t - \mathbf{TH}_{jr}^{up} + 1, t - 1] \\ z_{jrt} &\leq 1 + z_{jrc} - z_{jr,c-1}, c \in [t - \mathbf{TH}_{jr}^{down} + 1, t - 1] \end{aligned} \quad (3.12)$$

where:

- $\mathbf{TH}_{jr}^{up(down)}$ minimum up(down)time of hydro unit j and plant r (h).

It is expected during the real time operation that large hydro plants do not turn on/off often, but depending on the planning horizon and on the minimum up (down)time of the hydro units, this may happen. Thus, in order to avoid many start-ups, a constraint to define a maximum number of start-ups is used for the hydro units, as expressed in the equation (3.13).

$$\begin{aligned} y_{jrt} &\geq z_{jrt} - z_{jr,t-1}, \\ \sum_{t=1}^T y_{jrt} &\leq \mathbf{NS}_{jr}, \\ y_{jrt} &\geq 0, \end{aligned} \quad (3.13)$$

where:

y_{jrt}	auxiliary variable to compute the number of start-ups of hydro unit j , plant r , and stage t ;
\mathbf{NS}_{jr}	maximum startups of the unit j and plant r .

One of the key issues regarding UC is the HPF, which is a nonlinear and nonconvex function due to the nature of the hydroelectric losses, efficiency, net head, and other aspects. Moreover, there are forbidden zones associated with vibrations in the turbine shaft. In this sense, it is a great challenge to represent HPF properly since this representation needs to be computationally efficient but also detailed enough so that the solution obtained is practical. Linear representations of the HPF are used broadly since this representation is especially useful considering computational efforts and details of the hydro units. The procedure to build a piecewise linear function can be accomplished through the Convex Hull algorithm. The details of this process can be seen on FREDO(2016). A piecewise linear representation of the HPF was used in this work, but firstly we present succinctly the nonlinear formulation of the HPF.

3.3.1 Nonlinear Hydro Power Function

The mathematical expression that defines the HPF for a unit j , hydro plant r , and stage t is given by:

$$ph_{jrt} = \mathbf{G} \cdot \eta_{jrt} \cdot h_{jrt} \cdot q_{jrt} \quad (3.14)$$

where:

ph_{jrt}	power generation of the unit j , plant r and stage t (MW);
\mathbf{G}	constant value of 0.00981 (MW/(m ³ /s)·m);
q_{jrt}	turbined outflow of the generating unit j , plant r and stage t (m ³ /s);
h_{jrt}	net head of the unit j , plant r and stage t (m);
$\eta(q, h)_{jrt}$	hydraulic efficiency unit j , plant r , and stage t .

Net head is defined using forebay and tailrace levels, besides the losses of each unit as follows:

$$h = fbl(v) - trl(w, s) - pl(q) \quad (3.15)$$

where:

$fbl(v)$	forebay level (m);
$trl(w,s)$	tailrace level (m);
$pl(q)$	hydraulic losses (m).

In the Brazilian case, the fbl and trl functions are expressed by the following fourth-degree polynomials:

$$fbl(v) = \mathbf{HM}_0 + \mathbf{HM}_1 \cdot v + \mathbf{HM}_2 \cdot v^2 + \mathbf{HM}_3 \cdot v^3 + \mathbf{HM}_4 \cdot v^4 \quad (3.16)$$

$$\begin{aligned} trl(w,s) = & \mathbf{HJ}_0 + \mathbf{HJ}_1 \cdot (w+s) + \mathbf{HJ}_2 \cdot (w+s)^2 \\ & + \mathbf{HJ}_3 \cdot (w+s)^3 + \mathbf{HJ}_4 \cdot (w+s)^4 \end{aligned} \quad (3.17)$$

where, $\mathbf{HM}_0, \dots, \mathbf{HM}_4$ and $\mathbf{HJ}_0, \dots, \mathbf{HJ}_4$ are the coefficients for fbl and trl , respectively. Equation (3.18) defines the hydraulic losses of the generating unit.

$$pl(q) = \mathbf{PR} \cdot q^2 \quad (3.18)$$

where \mathbf{PR} (s^2/m^5) is the constant of hydraulic losses. Finally, the unit efficiency is defined by the following polynomial:

$$\eta(q,h) = \mathbf{R}_0 + \mathbf{R}_1 \cdot q + \mathbf{R}_2 \cdot q^2 + \mathbf{R}_3 \cdot h + \mathbf{R}_4 \cdot h^2 + \mathbf{R}_5 \cdot q \cdot h \quad (3.19)$$

where, $\mathbf{R}_0, \dots, \mathbf{R}_5$ are coefficients of the efficiency equation.

Now, we present the piecewise linear functions that represent in an approximate way the nonlinear function HPF described above. We consider that units possess only one forbidden zone. Furthermore, it is also assumed that each hydro plant has identical units. Five different piecewise linear HPF models are presented in this work and they are named as DFm ($m = 1, 2, \dots, 5$).

3.3.2 Individual Model (DF1)

This section presents the formulation for the individual representation of the HPF. Firstly, we consider that the following linear piecewise model is available:

$$ph_{jrt} - \mathbf{C0}_{jr}^{(d)} q_{jrt} - \mathbf{C1}_{jr}^{(d)} h_{jrt} \leq \mathbf{C2}_{jr}^{(d)}, \quad d = 1, \mathbf{D}_{jr} \quad (3.20)$$

where:

ph_{jrt}	power of hydro unit j , plant r and stage t (MW);
$\mathbf{C}k_{jr}^{(d)}$	coefficient k of the hyperplane d that represents the piecewise linear HPF of the generating unit j and plant r ;
h_{jrt}	net head of hydro unit j , plant r and stage t (m);
\mathbf{D}_{jr}	number of hyperplanes that represents the piecewise linear HPF of the generating unit j and plant r .

It is known that net head is a nonlinear function of the forebay (fbl) and tailrace (trl) elevations, as well as the penstock hydraulic losses (pl). For using MILP formulation, a crucial aspect is that the functions representing the fbl , trl , and pl can be approximated by a linear or piecewise linear model. Indeed, linearity considerations for the fbl and trl functions are reasonable in the day-ahead operation scheduling. However, it is also possible to include a piecewise linear model for these functions in the proposed model, especially for the trl case, since this last has a greater impact in the short-term horizon when compared to the variation of the fbl . The pl is a convex function and it can be approximate precisely using the piecewise linear function.

Thus, considering that \mathbf{NG}_r generating units are available for operation in the hydro plant r , the individual model (DF1) of the HPF is given by the following mixed-integer formulation:

$$ph_{jrt} - \mathbf{C0}_{jr}^{(d)} q_{jrt} - \mathbf{C1}_{jr}^{(d)} h_{jrt} \leq \mathbf{C2}_{jr}^{(d)}, \quad d = 1, \mathbf{D}_{jr} \quad (3.21)$$

$$h_{jrt} - \mathbf{FB0}_r v_{rt} - \mathbf{FB1}_r + \mathbf{TL0}_r (w_{rt} + s_{rt}) + \mathbf{TL1}_r + pl_{jrt} = 0 \quad (3.22)$$

$$w_{rt} - \sum_{j=1}^{\mathbf{NG}_r} q_{jrt} = 0 \quad (3.23)$$

$$pl_{jrt} - \mathbf{D0}_{jr}^{(e)} q_{jrt} \geq \mathbf{D1}_{jr}^{(e)} z_{jrt}, \quad e = 1, \mathbf{E}_{jr} \quad (3.24)$$

$$z_{jrt} \mathbf{Q}_{jr}^{\min} \leq q_{jrt} \leq \mathbf{Q}_{jr}^{\max} z_{jrt} \quad (3.25)$$

$$z_{jrt} \mathbf{PH}_{jr}^{\min} \leq ph_{jrt} \leq \mathbf{PH}_{jr}^{\max} z_{jrt} \quad (3.26)$$

where:

$\mathbf{FB}k_r$	coefficient k that represents the linear approximation of the forebay elevation of the hydro plant r ;
$\mathbf{TL}k_r$	coefficient k that represents the linear approximation of the tailrace elevation of the hydro plant r ;
pl_{jrt}	penstock hydraulic loss of hydro unit j , plant r and stage t (m);
$\mathbf{D}k_{jr}^{(e)}$	coefficient k of the hyperplane e that represents the piecewise linear penstock hydraulic loss of the unit j and plant r ;
\mathbf{E}_{jr}	number of hyperplanes that represents the piecewise linear penstock hydraulic function of the unit j and plant r .
$\mathbf{PH}_{jr}^{\max(\min)}$	Maximum (minimum) power of hydro unit j and plant r ;

3.3.3 Individual Model with Equal Generation (DF2)

It is known from the optimality conditions that, in the optimal solution, the identical units in the same hydro plant must have same generation level, which means equals values of turbined outflow, efficiency, and net head. However, the DF1 model does not guarantee this condition, since the solution is associated with extreme points of the feasible set composed by inequality and equality constraints. Thus, the equation (3.27) is added to the DF1 model to create an individual model with equal generation, which is defined in this work as DF2 model.

$$0 \leq qct_{rt} - q_{jrt} \leq \mathbf{Q}_{jr}^{\max} (1 - z_{jrt}) \quad (3.27)$$

where:

qct_{rt} auxiliary variable of hydro plant r and stage t (m^3/s).

Therefore, the DF2 formulation is the one presented for DF1 in addition to the equation (3.27).

3.3.4 Individual Model with Aggregated Constraints (DF3)

The main idea in this section is, instead of using a piecewise linear model for each unit explicitly, we represent a group of identical units by a single piecewise HPF. To simplify the mathematical notation, this work considers plants in which all units are identical. Nevertheless, the notation can be easily extended for cases with distinct groups of identical units. The goal with this aggregation is to decrease the number of constraints associated to the HPF, which will be seen that also decreases reasonably the number of constraints for the HTUC problem.

Firstly, we can rewrite the equation (3.20) as follows:

$$ph_{jt} - \mathbf{C0}_{jr}^{(d)} q_{jt} - \mathbf{C1}_{jr}^{(d)} (gh_{rt} - pl_{jt}) z_{jt} \leq \mathbf{C2}_{jr}^{(d)} z_{jt}, d = 1, \mathbf{D}_{jr} \quad (3.28)$$

where gh_{rt} is the gross head of hydro plant r and stage t (m). When assuming \mathbf{NG}_r units to be identical, we can aggregate the inequalities constraints, resulting in the following piecewise linear model with \mathbf{D}_{jr} constraints:

$$\begin{aligned} & ph_{rt} - \mathbf{C0}_{jr}^{(d)} \sum_{j=1}^{\mathbf{NG}_r} z_{jt} q_{jt} - \mathbf{C1}_{jr}^{(d)} \sum_{j=1}^{\mathbf{NG}_r} z_{jt} (gh_{rt} - pl_{jt}) \\ & \leq \mathbf{C2}_{jr}^{(d)} \sum_{j=1}^{\mathbf{NG}_r} z_{jt}, d = 1, \mathbf{D}_{jr} \end{aligned} \quad (3.29)$$

As shown above, the equation possesses the following nonlinearities: $z_{jt} \cdot q_{jt}$, $z_{jt} \cdot gh_{rt}$, and $z_{jt} \cdot pl_{jt}$. The first and the latter nonlinearities can be handled indirectly via constraints of maximum/minimum turbined out-flows and hydraulic losses. Thus, (3.29) is equivalent to:

$$\begin{aligned} & ph_{rt} - \mathbf{C0}_{jr}^{(d)} \sum_{j=1}^{\mathbf{NG}_r} q_{jt} - \mathbf{C1}_{jr}^{(d)} \sum_{j=1}^{\mathbf{NG}_r} z_{jt} gh_{rt} + \mathbf{C1}_{jr}^{(d)} \sum_{j=1}^{\mathbf{NG}_r} pl_{jt} \\ & \leq \mathbf{C2}_{jr}^{(d)} \sum_{j=1}^{\mathbf{NG}_r} z_{jt}, d = 1, \mathbf{D}_{jr}. \end{aligned} \quad (3.30)$$

The nonlinearity $z_{jt} \cdot gh_{rt}$ can be addressed using the auxiliary variable $gha_{jt} = z_{jt} \cdot gh_{rt}$ and by including the following constraints:

$$\mathbf{GH}_r^{\min} z_{jt} \leq gha_{jt} \leq \mathbf{GH}_r^{\max} z_{jt}, \quad (3.31)$$

$$\mathbf{GH}_r^{\min} (1 - z_{jt}) \leq gh_{rt} - gha_{jt} \leq \mathbf{GH}_r^{\max} (1 - z_{jt}), \quad (3.32)$$

where:

$\mathbf{GH}_r^{\min, \max}$ Minimum (maximum) value of the gross head of the hydro plant r (m).

Thus, the constraints (3.30) can be rewritten as:

$$\begin{aligned} & ph_{rt} - \mathbf{C0}_{jr}^{(d)} \sum_{j=1}^{\mathbf{NG}_r} q_{jt} - \mathbf{C1}_{jr}^{(d)} \sum_{j=1}^{\mathbf{NG}_r} gha_{jt} + \mathbf{C1}_{jr}^{(d)} \sum_{j=1}^{\mathbf{NG}_r} pl_{jt} \\ & \leq \mathbf{C2}_{jr}^{(d)} \sum_{j=1}^{\mathbf{NG}_r} z_{jt}, d = 1, \mathbf{D}_{jr}, \end{aligned} \quad (3.33)$$

$$\mathbf{GH}_r^{\min} z_{jt} \leq gha_{jt} \leq \mathbf{GH}_r^{\max} z_{jt},$$

$$\mathbf{GH}_r^{\min} (1 - z_{jt}) \leq gh_{rt} - gha_{jt} \leq \mathbf{GH}_r^{\max} (1 - z_{jt}).$$

To finish the DF3 model, we include in (3.33) the equations associated with the hydraulic loss and gross head shown previously. As a result, the DF3 model is given by the following constraints:

$$\begin{aligned}
& ph_{rt} - \mathbf{C0}_{jr}^{(d)} \sum_{j=1}^{\mathbf{NG}_r} q_{jrt} - \mathbf{C1}_{jr}^{(d)} \sum_{j=1}^{\mathbf{NG}_r} gha_{jrt} + \mathbf{C1}_{jr}^{(d)} \sum_{j=1}^{\mathbf{NG}_r} pl_{jrt} \\
& \leq \mathbf{C2}_{jr}^{(d)} \sum_{j=1}^{\mathbf{NG}_r} z_{jrt}, d = 1, \mathbf{D}_{jr}, \\
& \mathbf{GH}_r^{\min} z_{jrt} \leq gha_{jrt} \leq \mathbf{GH}_r^{\max} z_{jrt}, \\
& \mathbf{GH}_r^{\min} (1 - z_{jrt}) \leq gh_{rt} - gha_{jrt} \leq \mathbf{GH}_r^{\max} (1 - z_{jrt}), \quad (3.34) \\
& gh_{rt} - \mathbf{FB0}_r v_{rt} - \mathbf{FB1}_r + \mathbf{TL0}_r (w_{rt} + s_{rt}) + \mathbf{TL1}_r = 0, \\
& w_{rt} - \sum_{j=1}^{\mathbf{NG}_r} q_{jrt} = 0, \\
& pl_{jrt} - \mathbf{D0}_{jr}^{(e)} q_{jrt} \geq \mathbf{D1}_{jr}^{(e)} z_{jrt}, e = 1, \mathbf{E}_{jr}, \\
& z_{jrt} \mathbf{Q}_{jr}^{\min} \leq q_{jrt} \leq \mathbf{Q}_{jr}^{\max} z_{jrt}.
\end{aligned}$$

3.3.5 Aggregated Units with one Binary Variable per Plant (DF4)

The HPF models presented previously represent each hydro unit individually in the problem. Thus, the number of binary variables is the same for all of them, even though the number of constraints is different for each model. It is known that binary variables are usually the complicated ones in MILP problems. To decrease the number of binary variables, an aggregated hydro model (DF4) is proposed, which uses only one binary variable per hydro plant, instead of per hydro unit such as the other models. Besides that, only one turbined outflow variable is used per plant. Thus, the aggregated hydro model (DF4) of the HPF is given by the following mixed-integer formulation:

$$\begin{aligned}
& ph_{rt} - \mathbf{CP0}_r^{(g)} w_{rt} - \mathbf{CP1}_r^{(g)} hp_{rt} \leq \mathbf{CP2}_r^{(d)}, g = 1, \mathbf{G}_r \\
& hp_{rt} - \mathbf{FB0}_r v_{rt} - \mathbf{FB1}_r + \mathbf{TL0}_r (w_{rt} + s_{rt}) + \mathbf{TL1}_r + plp_{rt} = 0 \\
& plp_{rt} - \mathbf{DP0}_r^{(l)} w_{rt} \geq \mathbf{DP1}_r^{(l)}, l = 1, \mathbf{L}_r \quad (3.35) \\
& z_{rt} \mathbf{QP}_r^{\min} \leq w_{rt} \leq \mathbf{QP}_r^{\max} z_{rt} \\
& z_{rt} \mathbf{PH}_r^{\min} \leq ph_{rt} \leq \mathbf{PH}_r^{\max} z_{rt}
\end{aligned}$$

where:

$\mathbf{CP}k_r^{(g)}$	coefficient k of the hyperplane g that represents the piecewise linear HPF of the plant r ;
hp_{rt}	net head of hydro plant r and stage t (m);
\mathbf{G}_r	number of hyperplanes that represents the piecewise linear HPF of the hydro plant r .
plp_{rt}	penstock hydraulic hydro plant r and stage t (m);
$\mathbf{DP}k_r^{(l)}$	coefficient k of the hyperplane l that represents the piecewise linear penstock hydraulic loss of the plant r ;
\mathbf{L}_r	number of hyperplanes that represents the piecewise linear penstock hydraulic function of the plant r .
$\mathbf{QP}_r^{\min,\max}$	Minimum (maximum) value of the turbined outflow of the hydro plant r (m^3/s);
z_{rt}	Binary variable of hydro plant r and stage t ;

Note that equation (3.35) includes the limits of the turbined outflow in the plant, where the minimum value corresponds to the minimum of a single unit, while its maximum corresponds to the maximum of the hydro plant. Additionally, model DF4 cannot precisely include the minimum up/downtime constraints. On the other hand, the model demands less computational effort since it has fewer variables and constraints than the other models presented above.

3.3.6 Aggregated Units without Binary Variable (DF5)

Model DF5 is the same that DF4, except that in DF5 binary variables for hydro plants are not used, which means that in the equation (3.36) the minimum turbined outflow is zero. Therefore, the minimum power generation is also zero as described in the equation below:

$$\begin{aligned}
ph_{rt} - \mathbf{CP0}_r^{(g)} w_{rt} - \mathbf{CP1}_r^{(g)} hp_{rt} &\leq \mathbf{CP2}_r^{(d)}, g = 1, \mathbf{G}_r \\
hp_{rt} - \mathbf{FB0}_r v_{rt} - \mathbf{FB1}_r + \mathbf{TL0}_r (w_{rt} + s_{rt}) + \mathbf{TL1}_r + plp_{rt} &= 0 \\
plp_{rt} - \mathbf{DP0}_r^{(l)} w_{rt} &\geq \mathbf{DP1}_r^{(l)}, l = 1, \mathbf{L}_r \\
0 \leq w_{rt} &\leq \mathbf{QP}_r^{\max} \\
0 \leq ph_{rt} &\leq \mathbf{PH}_r^{\max}
\end{aligned} \tag{3.36}$$

3.4 Hydrothermal Unit Commitment Model

This section presents the deterministic optimization model for the Hydrothermal Unit Commitment (HTUC) problem. The model below considers the individual representation of the HPF, i.e., DF1 model.

$$\min \sum_{i=1}^{NT} \sum_{t=1}^T (\mathbf{C}_i \cdot pt_{it} + \mathbf{FC}_i \cdot u_{it} + sc_{it}) + \sum_{b=1}^B \sum_{t=1}^T (\mathbf{AC}_b \cdot pd_{bt}) + \alpha \quad (3.37)$$

s.t.:

$$-\mathbf{FL}_l^{\max} \leq \sum_{b=1}^B \Gamma_{lb} \left(\sum_{r \in \mathbf{R}_b} ph_{rt} + \sum_{i \in \mathbf{I}_b} pt_{it} + \sum_{g \in \mathbf{RW}_b} \mathbf{PW}_{gt} + pd_{bt} - \mathbf{L}_{bt} \right) \leq \mathbf{FL}_l^{\max} \quad (3.38)$$

$$\sum_{b=1}^B \sum_{r \in \mathbf{R}_b} ph_{rt} + \sum_{b=1}^B \sum_{i \in \mathbf{I}_b} pt_{it} + \sum_{b=1}^B \sum_{g \in \mathbf{RW}_b} \mathbf{PW}_{gt} + \sum_{b=1}^B pd_{bt} = \sum_{b=1}^B \mathbf{L}_{bt} \quad (3.39)$$

$$sc_{it} \geq (u_{it} - u_{i,t-1}) \cdot \mathbf{SC}_i, \quad sc_{it} \geq 0, \quad (3.40)$$

$$pt_{i,t-1} \leq pt_{it} + u_{it} \mathbf{R}_i^{\text{down}} + (1 - u_{it}) \mathbf{GT}_i^{\min} \quad (3.41)$$

$$pt_{it} \leq pt_{i,t-1} + u_{i,t-1} \mathbf{R}_i^{\text{up}} + (1 - u_{i,t-1}) \mathbf{GT}_i^{\min} \quad (3.42)$$

$$u_{it} \geq u_{ic} - u_{i,c-1}, \quad c \in [t - \mathbf{TT}_i^{\text{up}} + 1, t - 1], \quad (3.43)$$

$$u_{it} \leq 1 + u_{ic} - u_{i,c-1}, \quad c \in [t - \mathbf{TT}_i^{\text{down}} + 1, t - 1],$$

$$\mathbf{PT}_i^{\min} u_{it} \leq pt_{it} \leq \mathbf{PT}_i^{\max} u_{it} \quad (3.44)$$

$$y_{jrt} \geq z_{jrt} - z_{j,r,t-1}, \quad \sum_{t=1}^T y_{jrt} \leq \mathbf{NS}_{jr}, \quad y_{jrt} \geq 0, \quad (3.45)$$

$$z_{jrt} \geq z_{jrc} - z_{j,r,c-1}, \quad c \in [t - \mathbf{TH}_{jr}^{\text{up}} + 1, t - 1] \quad (3.46)$$

$$z_{jrt} \leq 1 + z_{jrc} - z_{j,r,c-1}, \quad c \in [t - \mathbf{TH}_{jr}^{\text{down}} + 1, t - 1]$$

$$w_{rt} = \sum_{j=1}^{NG_r} q_{jrt} \quad (3.47)$$

$$v_{rt} - v_{r,t-1} + \mathbf{C}_1 \left[w_{rt} + s_{rt} - \sum_{m \in \mathcal{V}_r^{\text{op}}} (w_{m,t-\Omega_{mr}} + s_{m,t-\Omega_{mr}}) + \mathbf{Y}_{rt} \right] = 0 \quad (3.48)$$

$$\alpha + \sum_{r=1}^{n_r} \boldsymbol{\pi}_r^{(g)} v_{rT} \geq \Lambda^{(g)} \quad (3.49)$$

$$\mathbf{V}_r^{\min} \leq v_{rt} \leq \mathbf{V}_r^{\max}, \quad s_{rt} \leq \mathbf{S}_r^{\max} \quad (3.50)$$

$$ph_{jrt} - \mathbf{C0}_{jr}^{(d)} q_{jrt} - \mathbf{C1}_{jr}^{(d)} h_{jrt} \leq \mathbf{C2}_{jr}^{(d)}, \quad d = 1, \mathbf{D}_{jr} \quad (3.51)$$

$$h_{jrt} - \mathbf{FB0}_r v_{rt} - \mathbf{FB1}_r + \mathbf{TL0}_r (w_{rt} + s_{rt}) + \mathbf{TL1}_r + pl_{jrt} = 0$$

$$pl_{jrt} - \mathbf{D0}_{jr}^{(e)} q_{jrt} \geq \mathbf{D1}_{jr}^{(e)} z_{jrt}, e = 1, \mathbf{E}_{jr} \quad (3.52)$$

$$z_{jrt} \mathbf{PH}_{jr}^{\min} \leq ph_{jrt} \leq \mathbf{PH}_{jr}^{\max} z_{jrt} \quad (3.53)$$

$$z_{jrt} \mathbf{Q}_{jr}^{\min} \leq q_{jrt} \leq \mathbf{Q}_{jr}^{\max} z_{jrt}$$

where:

- NT** number of thermal plants;
- AC_b** deficit unitary cost of the bus *b* (R\$/MWh);
- pd_{bt}** deficit in bus *b* and stage *t* (MW).

The objective function (3.37) aims to minimize the operating cost. Constraints (3.38) and (3.39) are the classical DC power flow equations. Equations (3.40) - (3.44) correspond to the constraints that represent start-up cost, ramp down/up, minimum up/downtime and generation limits of the thermal plants. The set (3.45) - (3.50) refer to the hydro plants constraints given by, respectively, maximum number of start-ups of units, minimum up/down times, water balance in the penstock, streamflow balance in the reservoirs, future cost function, and limits on volumes and spillage of the reservoirs. In turn, equations (3.51) - (3.53) correspond to the individual HPF model (DF1).

To formulate the other deterministic HTUC problems, the equations (3.51) - (3.53) are altered to consider DF2, DF3, DF4 and DF5 models. For instance, to obtain the model DF2, it is only necessary the addition of equation (3.27) in (3.37) - (3.53). On the other hand, to obtain model DF3 one must replace (3.51) - (3.53) by (3.34). The model DF4 is attained by substituting equations (3.51) - (3.53) by (3.35). Finally, as stated above, to obtain the model DF5 one has to replace equations (3.51) - (3.53) by (3.36).

To show the differences among the dimensions of the deterministic models, consider a system with **NT** thermal plants and a transmission system with **B** buses and **L** transmission lines, **NH** hydro plants, each one of these with **NG** identical units. Each unit has an HPF model with **D** piecewise linear approximations. Consider also that the FCF model has **F** piecewise linear approximations, and the planning horizon possesses **T** time stages. In this context, Table 3-1 presents the general expressions to calculate the number of constraints (equality and inequality) (without considering minimum up/downtime constraints, since these ones depend on the minimum up/downtime of each generating unit) and variables (binaries and continuous) for each UC model used in this the-

sis. In general terms, DF2 is the model that has the most constraints and variables, while DF5 has the fewest ones.

Table 3-1 - Constraints in the deterministic HTUC models.

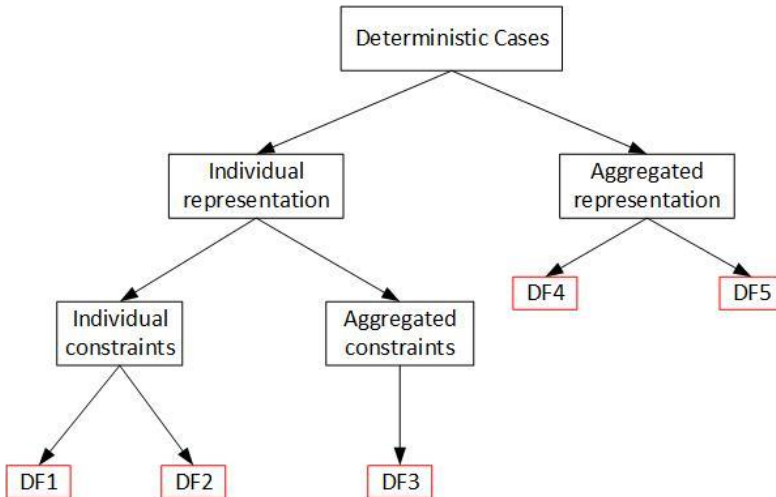
Model	Equality	Inequality
DF1	$T \cdot [NH \cdot (NG+2)+1]$	$NH \cdot NG \cdot T \cdot (P+D+4)+NT \cdot T \cdot (L+4)+F+2T$
DF2	$T \cdot [NH \cdot (NG+2)+1]$	$NH \cdot NG \cdot T \cdot (P+D+5)+NT \cdot T \cdot (L+4)+F+2T$
DF3	$T \cdot [NH \cdot (NG+2)+1]$	$NH \cdot NG \cdot T \cdot (P+5)+NT \cdot T \cdot (L+4)+F+2T+NH \cdot D \cdot T$
DF4	$T \cdot (3NH+1)$	$NH \cdot T \cdot (P+5)+NT \cdot T \cdot (L+4)+F+2T+NH \cdot D \cdot T$
DF5	$T \cdot (3NH+1)$	$NH \cdot T \cdot (P+5)+NT \cdot T \cdot (L+4)+F+2T+NH \cdot D \cdot T$

Table 3-2 - Variables in the deterministic HTUC models.

Model	Continuous	Binary
DF1	$T \cdot [NH \cdot (4 \cdot NG+3)+2 \cdot NT+B]+1$	$T \cdot (NH \cdot NG+NT)$
DF2	$T \cdot [NH \cdot (4 \cdot NG+3)+2 \cdot NT+B]+1$	$T \cdot (NH \cdot NG+NT)$
DF3	$T \cdot [NH \cdot (4 \cdot NG+3)+2 \cdot NT+B]+1$	$T \cdot (NH \cdot NG+NT)$
DF4	$T \cdot (7 \cdot NH+2 \cdot NT+B)+1$	$T \cdot (NH+NT)$
DF5	$T \cdot (7 \cdot NH+2 \cdot NT+B)+1$	$T \cdot NT$

Furthermore, Figure 3-1 shows a didactic tree to distinguish the differences among the deterministic cases.

Figure 3-1 - Deterministic cases and characteristics.



4. THE HYDROTHERMAL UNIT COMMITMENT PROBLEM VIA TWO-STAGE STOCHASTIC PROGRAMMING

As detailed previously, the HTUC is a key operational problem in power systems used to determine an optimal daily generation commitment schedule. Incorporating uncertainty in this already difficult mixed-integer optimization problem introduces significant computational challenges. Most existing stochastic UC and HTUC models consider either a two-stage decision structure, where the commitment schedule for the entire planning horizon is decided before the uncertainty is realized, or a multistage stochastic programming model with simplistic stochastic processes to ensure tractability. Although the focus of this work is the two-stage approach, firstly this chapter presents the main approaches for optimization under uncertainty. Next, multi and two-stage optimization are briefly described. Finally, Benders Decomposition (BD) and proximal bundle method, which are the methods used to solve the two-stage stochastic HTUC problem in this work, are discussed.

4.1 Methods for Optimization under Uncertainty

The data used as input information in any sort of problem is very important, since this may have measure errors, noise, or even be difficult to forecast with reasonable accuracy or precision. In this sense, there are two types of optimization problems according to the way the input is treated: deterministic optimization and optimization under uncertainty. The first one considers that the input data is known, while the second one considers it as a range of possibilities, and each one of these has a probability associated with. In this work, the uncertainty is related to the wind power generation, since there is a reasonable distinction in the costs and decisions when different wind scenarios are considered in the HTUC problem.

The main optimization-based approaches used to handle uncertainty comprise Robust Optimization (RO), Chance-Constrained Optimization (CCO) and Stochastic Optimization (SO) (TAHANAN, et al., 2018). RO uses the notion of uncertainty set, which basically reunites the adverse events which are not desired to have influence over the problem solution. RO is an interval-based optimization method in which, instead of scenarios, the uncertainty is specified via intervals. Moreover, RO makes no assumption on the probability density function (PDF) of the uncertain parameter, which is a very desirable feature if the PDF is not

well known (SHAFIEE, et al., 2017). More information about RO can be seen in the work of Ben-Tal and Nemirovski (2000).

CCO appears as an alternative to balance cost and robustness. In this approach, the probability is considered on the modeling of the constraints, defined as probabilistic constraints. In the HTUC context, these constraints are usually those associated to load balance requirements and/or stream flow equations. Nonetheless, probabilistic constraints of CCO can be nonconvex and hard to evaluate, which may increase computation time. There is a link between RO and CCO, which is to select an uncertainty set in such a way as to enforce a probabilistic constraint (BEN-TAL & NEMIROVSKI, 2009), so that the solutions coming from the RO method are compared with those coming from the CCO one. Moreover, one may aim at replacing the probabilistic constraint with a convex, although possibly more restrictive, constraint. More information concerning CCO can be seen in (DENTCHEVA, 2009).

At last, SO, also known as scenario tree approach, has been the subject of intense research in the last years in the UC context. The key advantage of using scenario trees is that uncertainty is assumed to be known in each node of the tree, which allows SO to be solved as a large-scale deterministic problem discretized on the tree. Thus, any technique used to solve deterministic problems might be used here. However, depending on the problem and if uncertainty is not well known for each node of the tree, there may be difficult issues related to determining the PDF of uncertain variables and generating the tree. These two subjects may be extremely complicated since it involves a wide range of techniques, and is not within the scope of this work. Thus, it is considered that the wind PDF is well known and also that the size of the scenario tree size is adequate to the HTUC problem. The SO technique may be classified according to the number of stages used in the problem: two or multi-stage. Each “stage” is composed by partial information or decisions of the whole problem as will be seen in the next sections.

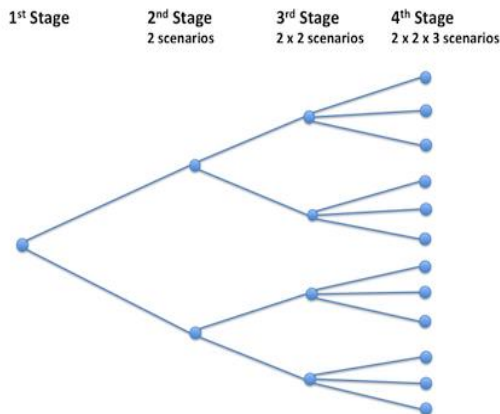
4.2 Multi-stage Stochastic Optimization

Multi-stage problems are present in a wide range of fields, such as engineering, financial planning, economic policy and many other applications, including the hydrothermal generation scheduling problem. These sorts of problem usually contain a very high level of uncertainty and they should be divided into a substantial set of scenarios, which might increase enormously the problem dimension and computational burden. To make the problem easier to handle, it is possible to divide it

into stages. Each stage is supposed to solve “a piece” of the problem, i.e., the problem itself can be solved partly by each stage, passing along valuable information for the next stages. In general, the decision maker solves the first stage and the decisions are transmitted to the second stage together with random events that also have influence over the second-stage decisions. Then, these ones are again passed to the next stage, usually with the presence of randomness, until the last stage is solved. After this process, the dual variables of the last stage are used to add an optimality cut to the previous stage, which is solved and its lagrange multipliers compose another optimality cut that is added to the preceding stage again. This entire process of forward/backward goes on until the solution is reached when a specific convergence is obtained. If the entire problem is modeled as a deterministic equivalent (DE), then all stages are solved simultaneously usually through a MILP technique.

Partitioning a problem into more than two stages is done typically for those problems that involve much randomness, and usually demands a reasonable computational effort. Figure 4-1 depicts an illustration of a scenario tree with four stages. Thus, a single hard problem can be split among smaller problems that can be solved, in general, with less effort than the original one.

Figure 4-1 – Scenario Tree.

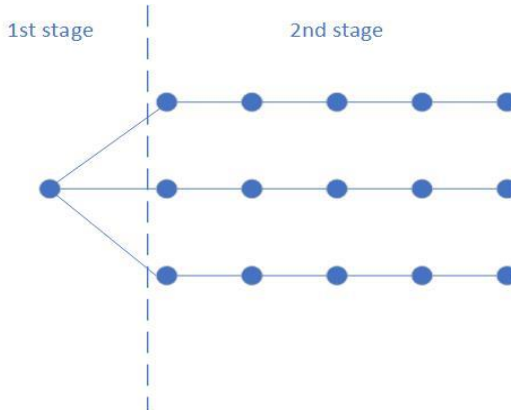


4.3 Two-stage Stochastic Optimization

Two-stage problems are, in general, easier to handle in comparison to multi-stage ones due to its efficiency and simplicity for having only two stages. It is important to emphasize that stage and time period are

not equivalent. The first one is related to the decisions taken and the second to the planning horizon. Figure 4-2 shows a tree divided only in two stages. The circles represent each time period, and then we see that in the second stage there are more than one time period in the same stage.

Figure 4-2 - Two-stage Tree.



Consequently, this model has been used broadly and the two-stage SO is used in this work to model the stochastic HTUC problem. The first stage decisions are composed by the binary variables, i.e., which generating units must be turned on/off. The second stage decisions are the power generated by each of these units. The randomness is present in the wind generation in the system described in chapter 5, which has a few wind farms positioned in some buses.

Two-stage problems can be written as a DE model. The DE considers the entire uncertain space simultaneously in only one optimization problem, which, in general, results in a large-scale one. However, this formulation is useful to show the variables associated with each scenario. In the next section, it is presented the DE formulation related to the HTUC problem for different representations of the HPF.

4.3.1 Stochastic model 1 – SF1

The SF1 HTUC model is based on the DF3, where the constraints of the individual HPF are aggregated. Thus, considering a tree with NC wind generation scenarios, each one with probability P_{ω} , the DE model associated with SF1 is given by:

$$\min \sum_{i=1}^{\text{NT}} \sum_{t=1}^{\text{T}} (\mathbf{FC}_i \cdot u_{it} + sc_{it}) + \sum_{\omega=1}^{\text{NC}} \mathbf{P}_\omega \left[\sum_{i=1}^{\text{NT}} \sum_{t=1}^{\text{T}} \mathbf{C}_i \cdot pt_{it\omega} + \sum_{b=1}^{\text{B}} \sum_{t=1}^{\text{T}} (\mathbf{AC}_b \cdot pd_{bt\omega}) + \alpha_\omega \right] \quad (4.1)$$

s.t.:

$$sc_{it} \geq (u_{it} - u_{i,t-1}) \cdot \mathbf{SC}_i, \quad sc_{it} \geq 0, \quad (4.2)$$

$$u_{it} \geq u_{ic} - u_{i,c-1}, \quad c \in [t - \mathbf{TT}_i^{\text{up}} + 1, t - 1], \quad (4.3)$$

$$u_{it} \leq 1 + u_{ic} - u_{i,c-1}, \quad c \in [t - \mathbf{TT}_i^{\text{down}} + 1, t - 1], \quad (4.3)$$

$$y_{jrt} \geq z_{jrt} - z_{jr,t-1}, \quad \sum_{t=1}^{\text{T}} y_{jrt} \leq \mathbf{NS}_{jr}, \quad y_{jrt} \geq 0, \quad (4.4)$$

$$z_{jrt} \geq z_{jrc} - z_{jr,c-1}, \quad c \in [t - \mathbf{TH}_{jr}^{\text{up}} + 1, t - 1] \quad (4.5)$$

$$z_{jrt} \leq 1 + z_{jrc} - z_{jr,c-1}, \quad c \in [t - \mathbf{TH}_{jr}^{\text{down}} + 1, t - 1] \quad (4.5)$$

$$-\mathbf{FL}_l^{\max} \leq \sum_{b=1}^{\text{B}} \mathbf{\Gamma}_{lb} \left(\sum_{r \in \mathbf{R}_b} ph_{rt\omega} + \sum_{i \in \mathbf{I}_b} pt_{it\omega} + \sum_{g \in \mathbf{RW}_b} \mathbf{PW}_{gt\omega} + pd_{bt\omega} - \mathbf{L}_{bt} \right) \leq \mathbf{FL}_l^{\max} \quad (4.6)$$

$$\sum_{b=1}^{\text{B}} \sum_{r \in \mathbf{R}_b} ph_{rt\omega} + \sum_{b=1}^{\text{B}} \sum_{i \in \mathbf{I}_b} pt_{it\omega} + \sum_{b=1}^{\text{B}} \sum_{g \in \mathbf{RW}_b} \mathbf{PW}_{gt\omega} + \sum_{b=1}^{\text{B}} pd_{bt\omega} = \sum_{b=1}^{\text{B}} \mathbf{L}_{bt} \quad (4.7)$$

$$pt_{i,t-1,\omega} \leq pt_{it\omega} + u_{it} \mathbf{R}_i^{\text{down}} + (1 - u_{it}) \mathbf{GT}_i^{\min} \quad (4.8)$$

$$pt_{it\omega} \leq pt_{i,t-1,\omega} + u_{i,t-1} \mathbf{R}_i^{\text{up}} + (1 - u_{i,t-1}) \mathbf{GT}_i^{\min} \quad (4.9)$$

$$\mathbf{PT}_i^{\min} u_{it} \leq pt_{it\omega} \leq \mathbf{PT}_i^{\max} u_{it} \quad (4.10)$$

$$v_{rt\omega} - v_{r,t-1,\omega} + \mathbf{C}_1 \left[w_{rt\omega} + s_{rt\omega} - \sum_{m \in \mathcal{V}_r^{\text{up}}} (w_{m,t-\Omega_{mr},\omega} + s_{m,t-\Omega_{mr},\omega}) + \mathbf{Y}_{rt} \right] = 0 \quad (4.11)$$

$$\alpha_\omega + \sum_{r=1}^{n_r} \boldsymbol{\pi}_r^{(g)} v_{rT\omega} \geq \Lambda^{(g)} \quad (4.12)$$

$$\mathbf{V}_r^{\min} \leq v_{rt\omega} \leq \mathbf{V}_r^{\max}, \quad s_{rt\omega} \leq \mathbf{S}_r^{\max} \quad (4.13)$$

$$ph_{rt\omega} - \mathbf{C0}_{jr}^{(d)} \sum_{j=1}^{\text{NG}_r} q_{jrt\omega} - \mathbf{C1}_{jr}^{(d)} \sum_{j=1}^{\text{NG}_r} gha_{jrt\omega} + \mathbf{C1}_{jr}^{(d)} \sum_{j=1}^{\text{NG}_r} pl_{jrt\omega} \quad (4.14)$$

$$\leq \mathbf{C2}_{jr}^{(d)} \sum_{j=1}^{\text{NG}_r} z_{jrt}, \quad d = 1, \mathbf{D}_{jr},$$

$$\mathbf{GH}_r^{\min} z_{jrt} \leq gha_{jrt\omega} \leq \mathbf{GH}_r^{\max} z_{jrt}, \quad (4.15)$$

$$\mathbf{GH}_r^{\min} (1 - z_{jrt}) \leq gh_{rt\omega} - gha_{jrt\omega} \leq \mathbf{GH}_r^{\max} (1 - z_{jrt}), \quad (4.16)$$

$$w_{r\tau\omega} - \sum_{j=1}^{NG_r} q_{jr\tau\omega} = 0 \quad (4.17)$$

$$gh_{r\tau\omega} - \mathbf{FB0}_r v_{r\tau\omega} - \mathbf{FB1}_r + \mathbf{TL0}_r (w_{r\tau\omega} + s_{r\tau\omega}) + \mathbf{TL1}_r = 0, \quad (4.18)$$

$$pl_{jr\tau\omega} - \mathbf{D0}_{jr}^{(e)} q_{jr\tau\omega} \geq \mathbf{D1}_{jr}^{(e)} z_{jr}, e = 1, \mathbf{E}_{jr}, \quad (4.19)$$

$$z_{jr} \mathbf{Q}_{jr}^{\min} \leq q_{jr\tau\omega} \leq \mathbf{Q}_{jr}^{\max} z_{jr} \quad (4.20)$$

4.3.2 Stochastic Model – SF2

The stochastic HTUC model SF2 is based on the DF4 and aggregates hydro units using only one binary variable per hydro plant. Therefore, equations (4.21) - (4.24) below replace equations (4.14) - (4.20) in the model SF1. Thus, to obtain the DE for model SF2 we use equations (4.1) - (4.3), (4.6) - (4.13) in addition to equations (4.21) - (4.24).

$$ph_{r\tau\omega} - \mathbf{CP0}_r^{(g)} w_{r\tau\omega} - \mathbf{CP1}_r^{(g)} hp_{r\tau\omega} \leq \mathbf{CP2}_r^{(d)}, g = 1, \mathbf{G}_r \quad (4.21)$$

$$hp_{r\tau\omega} - \mathbf{FB0}_r v_{r\tau\omega} - \mathbf{FB1}_r + \mathbf{TL0}_r (w_{r\tau\omega} + s_{r\tau\omega}) + \mathbf{TL1}_r + plp_{r\tau\omega} = 0 \quad (4.22)$$

$$plp_{r\tau\omega} + \mathbf{DP0}_r^{(l)} w_{r\tau\omega} \geq \mathbf{DP1}_r^{(l)}, l = 1, \mathbf{L}_r \quad (4.23)$$

$$z_{rt} \mathbf{QP}_r^{\min} \leq w_{r\tau\omega} \leq \mathbf{QP}_r^{\max} z_{rt} \quad (4.24)$$

$$z_{rt} \mathbf{PP}_r^{\min} \leq ph_{r\tau\omega} \leq \mathbf{PP}_r^{\max} z_{rt}$$

4.3.3 Stochastic Model – SF3

The model SF3 is basically the same that SF2, except that binary variables are not used, i.e., in the equation (4.24) the minimum turbinéd outflow is zero and consequently, minimum generation is zero as well. Thus, the SF3 model is given by equations (4.1) - (4.3), (4.6) - (4.13) and (4.25) – (4.28).

$$ph_{r\tau\omega} - \mathbf{CP0}_r^{(g)} w_{r\tau\omega} - \mathbf{CP1}_r^{(g)} hp_{r\tau\omega} \leq \mathbf{CP2}_r^{(d)}, g = 1, \mathbf{G}_r \quad (4.25)$$

$$hp_{r\tau\omega} - \mathbf{FB0}_r v_{r\tau\omega} - \mathbf{FB1}_r + \mathbf{TL0}_r (w_{r\tau\omega} + s_{r\tau\omega}) + \mathbf{TL1}_r + plp_{r\tau\omega} = 0 \quad (4.26)$$

$$plp_{r\tau\omega} - \mathbf{DP0}_r^{(l)} w_{r\tau\omega} \geq \mathbf{DP1}_r^{(l)}, l = 1, \mathbf{L}_r \quad (4.27)$$

$$0 \leq w_{r\tau\omega} \leq \mathbf{QP}_r^{\max} z_{rt} \quad (4.28)$$

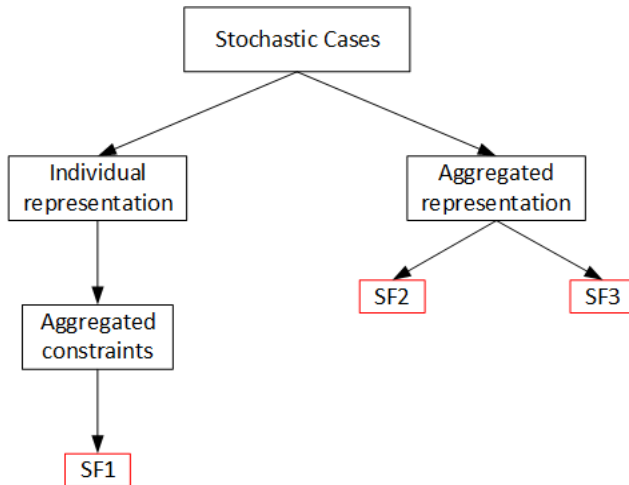
$$0 \leq ph_{r\tau\omega} \leq \mathbf{PP}_r^{\max} z_{rt}$$

Each DE HTUC formulation presented is a large-scale optimization problem and to solve them efficiently this work uses a decomposition technique. Within this framework, one of the most used decompositions in the UC problems is the BD, since the problem is suitable in the approach, i.e., we can split the entire set of variables into “easy” (continu-

ous) and “complicated” (binary) ones. Moreover, this technique has the advantage of supplying a feasible point, while dual methods (such as the LR), that are extremely used as well, cannot guarantee it. Furthermore, compared to MILP techniques, the BD approach is in general more efficient in terms of computational execution time (TAHANAN, et al., 2018). In this sense, we present the BD technique associated with the current HTUC problem.

To summarize the characteristics of each stochastic model, Figure 4-3 shows a tree comparing each model regarding their different representations.

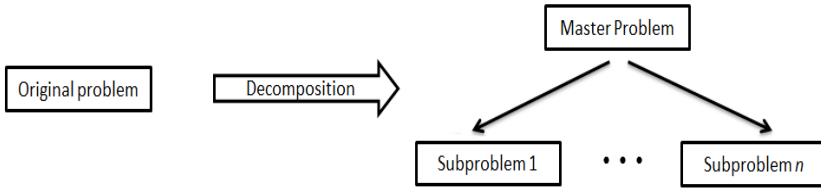
Figure 4-3 - Characteristics of the Stochastic cases.



4.4 Benders Decomposition

The BD was first proposed by Benders (1962) and has been widely used in a great variety of optimization problems, even though its application to UC problems is somewhat recent (TAHANAN, et al., 2018). The BD technique decomposes the original problem between master problem and different subproblems as shown in Figure 4-4.

Figure 4-4 - Benders Decomposition.



The general idea of the BD approach is to solve the master problem, which is composed mostly of binary variables, and then pass along these 0-1 variable values for the subproblems.

Next, these subproblems must be solved and their dual variables compose an optimality cut¹ that is added to the master problem. The master problem is then solved again with this new cut and this process continues until a specified convergence is reached. We detail the classical version of the DB algorithm considering the SF1 model, which is the most complete stochastic model presented in the previous section. The algorithm can be easily extended for the other models.

4.4.1 BD Algorithm

The algorithm below is built according to the specificities of this work.

1. Choose lower bound $LB^{(0)} = 0$, upper bound $UB^{(0)} = +\infty$, tolerance $tol > 0$. Set iteration $iter = 1$.
2. Solve the following master and consider $MVAL$ the value of its objective function. Equation (4.30) corresponds to the optimality cut added at iteration $iter > 1$. The process to obtain the cut is detailed ahead. In the next formulation, $\mathbf{U}_{it}^{(iter)}$, $\mathbf{Z}_{jrt}^{(iter)}$ are the value of

¹ It is important to highlight that, depending on the binary decisions supplied by the master problem, the second-stage subproblem can be infeasible. This aspect can occur in several operational conditions such as low initial level of reservoirs or when the maximum transmission lines capacity are reached. In this way, it would be necessary to use feasibility cuts; however, in this work we use an auxiliary variable to compute the deficit in all buses with load. In general, in order to avoid infeasibility, auxiliary variables are used in every single constraint of the problem. However, in this work specifically we noticed that only the deficit variables were in fact necessary. Therefore, the second-stage subproblems are always feasible, and then feasibility cuts are not needed.

the binary variables, $\mathbf{OF}_\omega^{(iter)}$ is the objective function of the subproblem ω , and $\lambda_{it\omega}^{(iter)}, \dots, \lambda_{it\omega}^{(iter)}, \beta_{jrt\omega}^{(iter)}, \dots, \beta_{jrt\omega}^{(iter)}$ are Lagrange multipliers obtained from the solution of the subproblems at iteration $iter$.

$$\min \sum_{i=1}^{NT} \sum_{t=1}^T (\mathbf{FC}_i \cdot u_{it} + sc_{it}) + \theta \quad (4.29)$$

$$\text{s.t.}: (4.2) - (4.5),$$

$$\begin{aligned} & \theta + \sum_{i=1}^{NT} \sum_{t=1}^T u_{it} \cdot \sum_{\omega=1}^{NC} \mathbf{P}_\omega \cdot \left[\lambda_{it\omega}^{(iter)} \cdot (\mathbf{GT}_i^{\min} - \mathbf{R}_i^{\text{down}}) + \right. \\ & \left. \lambda_{it\omega}^{(iter)} \cdot \mathbf{GT}_i^{\min} - \lambda_{it\omega}^{(iter)} \cdot \mathbf{GT}_i^{\max} \right] + \\ & \sum_{i=1}^{NT} \sum_{t=2}^T u_{i,t-1} \cdot \sum_{\omega=1}^{NC} \mathbf{P}_\omega \cdot \left[\lambda_{it\omega}^{(iter)} \cdot (\mathbf{GT}_i^{\min} - \mathbf{R}_i^{\text{up}}) \right] + \\ & \sum_{j=1}^{NG_r} \sum_{r=1}^{NR} \sum_{t=1}^T z_{jrt} \cdot \sum_{\omega=1}^{NC} \mathbf{P}_\omega \cdot \left(-\beta_{jrt\omega}^{(iter)} \cdot \mathbf{C}2_{jr}^{(d)} - \mathbf{GH}_r^{\max} \cdot \beta_{jrt\omega}^{(iter)} \right. \\ & \left. + \mathbf{GH}_r^{\min} \cdot \beta_{jrt\omega}^{(iter)} + \mathbf{GH}_r^{\max} \cdot \beta_{jrt\omega}^{(iter)} - \mathbf{GH}_r^{\min} \cdot \beta_{jrt\omega}^{(iter)} \right. \\ & \left. + \mathbf{D}1_{jr}^{(e)} \cdot \beta_{jrt\omega}^{(iter)} + \mathbf{Q}_{jr}^{\min} \cdot \beta_{jrt\omega}^{(iter)} - \mathbf{Q}_{jr}^{\max} \cdot \beta_{jrt\omega}^{(iter)} \right) \geq \sum_{\omega=1}^{NC} \mathbf{P}_\omega \cdot \left\{ \mathbf{OF}_\omega^{(iter)} \right. \\ & \left. + \sum_{i=1}^{NT} \sum_{t=1}^T \mathbf{U}_{it}^{(iter)} \cdot \left[\lambda_{it\omega}^{(iter)} \cdot (\mathbf{GT}_i^{\min} - \mathbf{R}_i^{\text{down}}) + \lambda_{it\omega}^{(iter)} \cdot \mathbf{GT}_i^{\min} - \lambda_{it\omega}^{(iter)} \cdot \mathbf{GT}_i^{\max} \right] \right. \\ & \left. + \sum_{i=1}^{NT} \sum_{t=2}^T \mathbf{U}_{i,t-1}^{(iter)} \cdot \left[\lambda_{it\omega}^{(iter)} \cdot (\mathbf{GT}_i^{\min} - \mathbf{R}_i^{\text{up}}) \right] + \sum_{t=1}^T \sum_{r=1}^{NR} \sum_{j=1}^{NG_r} \mathbf{Z}_{jrt}^{(iter)} \cdot \left(-\beta_{jrt\omega}^{(iter)} \cdot \mathbf{C}2_{jr}^{(d)} \right. \right. \\ & \left. \left. - \mathbf{GH}_r^{\max} \cdot \beta_{jrt\omega}^{(iter)} + \mathbf{GH}_r^{\min} \cdot \beta_{jrt\omega}^{(iter)} + \mathbf{GH}_r^{\max} \cdot \beta_{jrt\omega}^{(iter)} - \mathbf{GH}_r^{\min} \cdot \beta_{jrt\omega}^{(iter)} \right. \right. \\ & \left. \left. + \mathbf{D}1_{jr}^{(e)} \cdot \beta_{jrt\omega}^{(iter)} + \mathbf{Q}_{jr}^{\min} \cdot \beta_{jrt\omega}^{(iter)} - \mathbf{Q}_{jr}^{\max} \cdot \beta_{jrt\omega}^{(iter)} \right) \right\} \end{aligned} \quad (4.30)$$

3. Set $LB^{(iter)} = MVAL$. Use $\mathbf{U}_{it}^{(iter)} = u_{it}$ and $\mathbf{Z}_{jrt}^{(iter)} = z_{jrt}$ as an input data to solve the following subproblems associated with each scenario ω :

$$\min \sum_{i=1}^{NT} \sum_{t=1}^T \mathbf{C}_i \cdot pt_{it\omega} + \sum_{b=1}^B \sum_{t=1}^T (\mathbf{AC}_b \cdot pd_{bt\omega}) + \alpha_\omega \quad (4.31)$$

s.t: (4.6), (4.7), (4.11), (4.12), (4.14), (4.17), (4.18).

$$pt_{i,t-1,\omega} \leq pt_{it\omega} + \mathbf{U}_{it}^{(iter)} \mathbf{R}_i^{down} + (1 - \mathbf{U}_{it}^{(iter)}) \mathbf{GT}_i^{\min} \quad (4.32)$$

$$pt_{it\omega} \leq pt_{i,t-1,\omega} + \mathbf{U}_{i,t-1}^{(iter)} \mathbf{R}_i^{up} + (1 - \mathbf{U}_{i,t-1}^{(iter)}) \mathbf{GT}_i^{\min} \quad (4.33)$$

$$\mathbf{PT}_i^{\min} \mathbf{U}_{it}^{(iter)} \leq pt_{it\omega} \leq \mathbf{PT}_i^{\max} \mathbf{U}_{it}^{(iter)} \quad (4.34)$$

$$\mathbf{V}_r^{\min} \leq v_{rt\omega} \leq \mathbf{V}_r^{\max}, s_{rt\omega} \leq \mathbf{S}_r^{\max} \quad (4.35)$$

$$ph_{rt\omega} - \mathbf{C0}_{jr}^{(d)} \sum_{j=1}^{\mathbf{NG}_r} q_{jrt\omega} - \mathbf{C1}_{jr}^{(d)} \sum_{j=1}^{\mathbf{NG}_r} gha_{jrt\omega} + \mathbf{C1}_{jr}^{(d)} \sum_{j=1}^{\mathbf{NG}_r} pl_{jrt\omega} \leq \mathbf{C2}_{jr}^{(d)} \sum_{j=1}^{\mathbf{NG}_r} \mathbf{Z}_{jrt}^{(iter)}, d = 1, \mathbf{D}_{jr}, \quad (4.36)$$

$$\mathbf{GH}_r^{\min} \mathbf{Z}_{jrt}^{(iter)} \leq gha_{jrt\omega} \leq \mathbf{GH}_r^{\max} \mathbf{Z}_{jrt}^{(iter)}, \quad (4.37)$$

$$\mathbf{GH}_r^{\min} (1 - \mathbf{Z}_{jrt}^{(iter)}) \leq gh_{rt\omega} - gha_{jrt\omega} \leq \mathbf{GH}_r^{\max} (1 - \mathbf{Z}_{jrt}^{(iter)}), \quad (4.38)$$

$$gh_{rt\omega} - \mathbf{FB0}_r v_{rt\omega} - \mathbf{FB1}_r + \mathbf{TL0}_r (w_{rt\omega} + s_{rt\omega}) + \mathbf{TL1}_r = 0, \quad (4.39)$$

$$pl_{jrt\omega} + \mathbf{D0}_{jr}^{(e)} q_{jrt\omega} \geq \mathbf{D1}_{jr}^{(e)} \mathbf{Z}_{jrt\omega}^{(iter)}, e = 1, \mathbf{E}_{jr}, \quad (4.40)$$

$$\mathbf{Z}_{jrt}^{(iter)} \mathbf{Q}_{jr}^{\min} \leq q_{jrt\omega} \leq \mathbf{Q}_{jr}^{\max} \mathbf{Z}_{jrt}^{(iter)} \quad (4.41)$$

4. Obtain the upper bound of the problem that is given by:

$$UB^{(iter)} = \min \left(UB^{(iter-1)}, \sum_{i=1}^{\mathbf{NT}} \sum_{t=1}^{\mathbf{T}} (\mathbf{FC}_i \cdot u_{it}^{(iter)} + sc_{it}^{(iter)}) + \sum_{\omega=1}^{\mathbf{NC}} \mathbf{P}_{\omega} \cdot \mathbf{OF}_{\omega}^{(iter)} \right) \quad (4.42)$$

5. If $\left(\frac{UB^{(iter)} - LB^{(iter)}}{UB^{(iter)}} \right) \leq tol$, STOP.
6. Use $\mathbf{OF}_{\omega}^{(iter)}$, $\mathbf{U}_{it}^{(iter)}$, $\mathbf{Z}_{jrt}^{(iter)}$, $\lambda_{it\omega}^{(iter)}$, ..., $\lambda_{it\omega}^{(iter)}$, $\beta_{jrt\omega}^{(iter)}$, ..., $\beta_{jrt\omega}^{(iter)}$, to build an optimality cut that must be included in the master problem.
7. Set $iter = iter + 1$ and return to Step 2.

4.4.2 Optimality cut

Optimality cut is built based on the solutions of the second-stage subproblems in each iteration. To obtain this cut, it is necessary to use the Lagrange multipliers of each constraint that contain the coupling variables of the two-stage problem, which are the binary ones in this case. In this work, we add only one optimality cut for iteration, using the probabilities of each scenario to calculate an average cut. Thus, for the SF1 model, it is presented below the constraints that possess the first-stage variables and their respective dual variables.

$$\begin{aligned}
pt_{i,t-1,\omega} &\leq pt_{it\omega} + \mathbf{U}_{it} \mathbf{R}_i^{down} + (1 - \mathbf{U}_{it}) \mathbf{GT}_i^{\min} & \lambda \mathbf{1}_{it\omega} \\
pt_{it\omega} &\leq pt_{i,t-1,\omega} + \mathbf{U}_{i,t-1} \mathbf{R}_i^{up} + (1 - \mathbf{U}_{i,t-1}) \mathbf{GT}_i^{\min} & \lambda \mathbf{2}_{it\omega} \\
\mathbf{GT}_i^{\min} \mathbf{U}_{it} - pt_{it\omega} &\leq 0 & \lambda \mathbf{3}_{it\omega} \\
-\mathbf{GT}_i^{\max} \mathbf{U}_{it} + pt_{it\omega} &\leq 0 & \lambda \mathbf{4}_{it\omega}
\end{aligned} \tag{4.43}$$

$$\begin{aligned}
ph_{rt} - \mathbf{C0}_{jr}^{(d)} \sum_{j=1}^{NG_r} q_{jrt} - \mathbf{C1}_{jr}^{(d)} \sum_{j=1}^{NG_r} gha_{jrt} + \mathbf{C1}_{jr}^{(d)} \sum_{j=1}^{NG_r} pl_{jrt} & & \beta \mathbf{1}_{jrt\omega} \\
-\mathbf{C2}_{jr}^{(d)} \sum_{j=1}^{NG_r} \mathbf{Z}_{jrt} \leq 0, d = 1, \mathbf{D}_{jr}, & & \\
gha_{jrt} - \mathbf{GH}_r^{\max} \mathbf{Z}_{jrt} \leq 0 & & \beta \mathbf{2}_{jrt\omega} \\
\mathbf{GH}_r^{\min} \mathbf{Z}_{jrt} - gha_{jrt} \leq 0 & & \beta \mathbf{3}_{jrt\omega} \\
gh_{rt} - gha_{jrt} - \mathbf{GH}_r^{\max} (1 - \mathbf{Z}_{jrt}) \leq 0 & & \beta \mathbf{4}_{jrt\omega} \\
\mathbf{GH}_r^{\min} (1 - \mathbf{Z}_{jrt}) - gh_{rt} + gha_{jrt} \leq 0 & & \beta \mathbf{5}_{jrt\omega} \\
-pl_{jrt\omega} + \mathbf{D0}_{jr}^{(e)} \cdot q_{jrt\omega} + \mathbf{D1}_{jr}^{(e)} \cdot \mathbf{Z}_{jrt} \leq 0, e = 1, \mathbf{E}_{jr} & & \beta \mathbf{6}_{jrt\omega} \\
\mathbf{Z}_{jrt} \mathbf{Q}_{jr}^{\min} - q_{jrt\omega} \leq 0 & & \beta \mathbf{7}_{jrt\omega} \\
-\mathbf{Q}_{jr}^{\max} \mathbf{Z}_{jrt} + q_{jrt\omega} \leq 0 & & \beta \mathbf{8}_{jrt\omega}
\end{aligned} \tag{4.44}$$

The optimality cut is described by the following compact formulation:

$$\theta - \Theta \geq [\lambda \quad \beta] \begin{bmatrix} u - \mathbf{U} \\ z - \mathbf{Z} \end{bmatrix} \tag{4.45}$$

where,

- Θ expected value of the optimal costs associated with the second stage subproblems.
- λ vector with the expected values of the Lagrange multipliers associated with constraints (4.43).
- β vector with the expected values of the Lagrange multipliers associated with constraints (4.44).
- u vector with the binary variables associated with the thermal units;
- \mathbf{U} vector with the binary decisions provided by the master problem associated with thermal plants;
- z vector with binary variables associated with the hydro units;

\mathbf{Z} vector with binary decisions provided by the master problem associated with the hydro units.

The equation (4.45) can be rewritten as:

$$\theta - \lambda^t u - \beta^t z \geq \Theta - \lambda^t \mathbf{U} - \beta^t \mathbf{Z} \quad (4.46)$$

The value of Θ is obtained directly from the solution of the subproblems and is given by:

$$\Theta = \sum_{\omega=1}^{NC} \mathbf{P}_{\omega} \cdot \mathbf{O}\mathbf{F}_{\omega} \quad (4.47)$$

The next step is to determine, using the values of the Lagrange multipliers shown in (4.43) and (4.44), the expression of λ . Each component of this vector represents the derivative of the objective function of binary variables of the dual problem built from the dualization of the constraints (4.43) and (4.44). Thus, using this information, we obtain the following expression that details $\lambda^t u$ and $\lambda^t \mathbf{U}$:

$$\begin{aligned} \lambda^t u &= \sum_{i=1}^{NT} \sum_{t=1}^T u_{it} \cdot \left[\lambda 1_{it\omega} (\mathbf{G}\mathbf{T}_i^{\min} - \mathbf{R}_i^{\text{down}}) + \lambda 3_{it\omega} \mathbf{G}\mathbf{T}_i^{\min} - \lambda 4_{it\omega} \mathbf{G}\mathbf{T}_i^{\max} \right] \\ &+ \sum_{i=1}^{NT} \sum_{t=2}^T u_{i,t-1} \cdot \lambda 2_{it\omega} \cdot (\mathbf{G}\mathbf{T}_i^{\min} - \mathbf{R}_i^{\text{up}}) \end{aligned} \quad (4.48)$$

$$\begin{aligned} \lambda^t \mathbf{U} &= \sum_{i=1}^{NT} \sum_{t=1}^T \mathbf{U}_{it} \cdot \left[\lambda 1_{it\omega} (\mathbf{G}\mathbf{T}_i^{\min} - \mathbf{R}_i^{\text{down}}) + \lambda 3_{it\omega} \mathbf{G}\mathbf{T}_i^{\min} - \lambda 4_{it\omega} \mathbf{G}\mathbf{T}_i^{\max} \right] \\ &+ \sum_{i=1}^{NT} \sum_{t=2}^T \mathbf{U}_{i,t-1} \cdot \lambda 2_{it\omega} \cdot (\mathbf{G}\mathbf{T}_i^{\min} - \mathbf{R}_i^{\text{up}}) \end{aligned} \quad (4.49)$$

Likewise, we obtain the expression for the other terms that comprise (4.46):

$$\begin{aligned} \beta^t z &= \sum_{j=1}^{NG} \sum_{r=1}^{NR} \sum_{t=1}^T z_{jrt} \left(-\beta 1_{jrt\omega} \mathbf{C}2_{jr}^{(d)} - \mathbf{G}\mathbf{H}_r^{\max} \beta 2_{jrt\omega} + \mathbf{G}\mathbf{H}_r^{\min} \beta 3_{jrt\omega} \right. \\ &+ \left. \mathbf{G}\mathbf{H}_r^{\max} \beta 4_{jrt\omega} - \mathbf{G}\mathbf{H}_r^{\min} \beta 5_{jrt\omega} + \mathbf{D}1_{jr}^{(e)} \beta 6_{jrt\omega} + \mathbf{Q}_{jr}^{\min} \beta 7_{jrt\omega} - \mathbf{Q}_{jr}^{\max} \beta 8_{jrt\omega} \right) \end{aligned} \quad (4.50)$$

$$\beta^t \mathbf{Z} = \sum_{j=1}^{NG_r} \sum_{r=1}^{NR} \sum_{t=1}^T \mathbf{Z}_{jrt} \left(-\beta_{jrt} \mathbf{C}2_{jr}^{(d)} - \mathbf{G}H_r^{\max} \beta_{jrt} + \mathbf{G}H_r^{\min} \beta_{jrt} \right. \\ \left. + \mathbf{G}H_r^{\max} \beta_{jrt} - \mathbf{G}H_r^{\min} \beta_{jrt} + \mathbf{D}1_{jr}^{(e)} \beta_{jrt} + \mathbf{Q}_{jr}^{\min} \beta_{jrt} - \mathbf{Q}_{jr}^{\max} \beta_{jrt} \right) \quad (4.51)$$

Finally, we obtain the optimality cut (for only one scenario) in the equation (4.52), which is presented in the master problem formulated in (4.29) - (4.30).

$$\begin{aligned} & \theta + \sum_{i=1}^{NT} \sum_{t=1}^T u_{it} \cdot \left[\lambda_{1it} \cdot (\mathbf{G}T_i^{\min} - \mathbf{R}_i^{down}) + \right. \\ & \left. \lambda_{3it} \cdot \mathbf{G}T_i^{\min} - \lambda_{4it} \cdot \mathbf{G}T_i^{\max} \right] + \\ & \sum_{i=1}^{NT} \sum_{t=2}^T u_{i,t-1} \cdot \left[\lambda_{2it} \cdot (\mathbf{G}T_i^{\min} - \mathbf{R}_i^{up}) \right] + \\ & \sum_{j=1}^{NG_r} \sum_{r=1}^{NR} \sum_{t=1}^T z_{jrt} \cdot \left(-\beta_{jrt} \mathbf{C}2_{jr}^{(d)} - \mathbf{G}H_r^{\max} \cdot \beta_{jrt} \right. \\ & \left. + \mathbf{G}H_r^{\min} \cdot \beta_{jrt} + \mathbf{G}H_r^{\max} \cdot \beta_{jrt} - \mathbf{G}H_r^{\min} \cdot \beta_{jrt} \right. \\ & \left. + \mathbf{D}1_{jr}^{(e)} \cdot \beta_{jrt} + \mathbf{Q}_{jr}^{\min} \cdot \beta_{jrt} - \mathbf{Q}_{jr}^{\max} \cdot \beta_{jrt} \right) \geq \text{OF} \quad (4.52) \\ & + \sum_{i=1}^{NT} \sum_{t=1}^T U_{it} \cdot \left[\lambda_{1it} \cdot (\mathbf{G}T_i^{\min} - \mathbf{R}_i^{down}) + \lambda_{3it} \cdot \mathbf{G}T_i^{\min} - \lambda_{4it} \cdot \mathbf{G}T_i^{\max} \right] \\ & + \sum_{i=1}^{NT} \sum_{t=2}^T U_{i,t-1} \cdot \left[\lambda_{2it} \cdot (\mathbf{G}T_i^{\min} - \mathbf{R}_i^{up}) \right] + \sum_{j=1}^{NG_r} \sum_{r=1}^{NR} \sum_{t=1}^T \mathbf{Z}_{jrt} \cdot \left(-\beta_{jrt} \mathbf{C}2_{jr}^{(d)} \right. \\ & \left. - \mathbf{G}H_r^{\max} \cdot \beta_{jrt} + \mathbf{G}H_r^{\min} \cdot \beta_{jrt} + \mathbf{G}H_r^{\max} \cdot \beta_{jrt} - \mathbf{G}H_r^{\min} \cdot \beta_{jrt} \right. \\ & \left. + \mathbf{D}1_{jr}^{(e)} \cdot \beta_{jrt} + \mathbf{Q}_{jr}^{\min} \cdot \beta_{jrt} - \mathbf{Q}_{jr}^{\max} \cdot \beta_{jrt} \right) \} \end{aligned}$$

We generalize (4.52) for NC scenarios in the equation (4.53). The change is basically that for many scenarios we take into account the probability associated with each scenario.

$$\begin{aligned}
& \theta + \sum_{i=1}^{NT} \sum_{t=1}^T u_{it} \cdot \sum_{\omega=1}^{NC} \mathbf{P}_{\omega} \cdot \left[\lambda \mathbf{1}_{it\omega} \cdot (\mathbf{GT}_i^{\min} - \mathbf{R}_i^{\text{down}}) + \right. \\
& \left. \lambda \mathbf{3}_{it\omega} \cdot \mathbf{GT}_i^{\min} - \lambda \mathbf{4}_{it\omega} \cdot \mathbf{GT}_i^{\max} \right] + \\
& \sum_{i=1}^{NT} \sum_{t=2}^T u_{i,t-1} \cdot \sum_{\omega=1}^{NC} \mathbf{P}_{\omega} \cdot \left[\lambda \mathbf{2}_{it\omega} \cdot (\mathbf{GT}_i^{\min} - \mathbf{R}_i^{\text{up}}) \right] + \\
& \sum_{j=1}^{NG_r} \sum_{r=1}^{NR} \sum_{t=1}^T z_{jrt} \cdot \sum_{\omega=1}^{NC} \mathbf{P}_{\omega} \cdot (-\beta \mathbf{1}_{jrt\omega} \cdot \mathbf{C} \mathbf{2}_{jr}^{(d)} - \mathbf{GH}_r^{\max} \cdot \beta \mathbf{2}_{jrt\omega} \\
& + \mathbf{GH}_r^{\min} \cdot \beta \mathbf{3}_{jrt\omega} + \mathbf{GH}_r^{\max} \cdot \beta \mathbf{4}_{jrt\omega} - \mathbf{GH}_r^{\min} \cdot \beta \mathbf{5}_{jrt\omega} \\
& + \mathbf{D} \mathbf{1}_{jr}^{(e)} \cdot \beta \mathbf{6}_{jrt\omega} + \mathbf{Q}_{jr}^{\min} \cdot \beta \mathbf{7}_{jrt\omega} - \mathbf{Q}_{jr}^{\max} \cdot \beta \mathbf{8}_{jrt\omega}) \geq \sum_{\omega=1}^{NC} \mathbf{P}_{\omega} \cdot \{ \mathbf{O} \mathbf{F}_{\omega} \\
& + \sum_{i=1}^{NT} \sum_{t=1}^T \mathbf{U}_{it} \cdot \left[\lambda \mathbf{1}_{it\omega} \cdot (\mathbf{GT}_i^{\min} - \mathbf{R}_i^{\text{down}}) + \lambda \mathbf{3}_{it\omega} \cdot \mathbf{GT}_i^{\min} - \lambda \mathbf{4}_{it\omega} \cdot \mathbf{GT}_i^{\max} \right] \\
& + \sum_{i=1}^{NT} \sum_{t=2}^T \mathbf{U}_{i,t-1} \cdot \left[\lambda \mathbf{2}_{it\omega} \cdot (\mathbf{GT}_i^{\min} - \mathbf{R}_i^{\text{up}}) \right] + \sum_{j=1}^{NG_r} \sum_{r=1}^{NR} \sum_{t=1}^T \mathbf{Z}_{jrt} \cdot (-\beta \mathbf{1}_{jrt\omega} \cdot \mathbf{C} \mathbf{2}_{jr}^{(d)} \\
& - \mathbf{GH}_r^{\max} \cdot \beta \mathbf{2}_{jrt\omega} + \mathbf{GH}_r^{\min} \cdot \beta \mathbf{3}_{jrt\omega} + \mathbf{GH}_r^{\max} \cdot \beta \mathbf{4}_{jrt\omega} - \mathbf{GH}_r^{\min} \cdot \beta \mathbf{5}_{jrt\omega} \\
& + \mathbf{D} \mathbf{1}_{jr}^{(e)} \cdot \beta \mathbf{6}_{jrt\omega} + \mathbf{Q}_{jr}^{\min} \cdot \beta \mathbf{7}_{jrt\omega} - \mathbf{Q}_{jr}^{\max} \cdot \beta \mathbf{8}_{jrt\omega}) \}
\end{aligned} \tag{4.53}$$

The equation (4.53) shows the optimality cut for the SF1 model. For SF2, it is basically the same cut, but since there is only one binary variable per hydro plant, the summation of the hydro units is not used. The equation (4.54) shows the optimality cut for the SF2. Moreover, for SF3, the optimality cut has only the thermal part of the optimality cut, since there are not binary variables for hydro plants. The equation (4.55) shows the optimality cut for this model.

$$\begin{aligned}
& \theta + \sum_{t=1}^T \sum_{i=1}^{NT} u_{it} \cdot \sum_{\omega=1}^{NC} \mathbf{P}_{\omega} \cdot \left[\lambda_{1_{it\omega}} \cdot (\mathbf{GT}_i^{\min} - \mathbf{R}_i^{\text{down}}) + \right. \\
& \left. \lambda_{3_{it\omega}} \cdot \mathbf{GT}_i^{\min} - \lambda_{4_{it\omega}} \cdot \mathbf{GT}_i^{\max} \right] + \\
& \sum_{t=2}^T \sum_{i=1}^{NT} u_{i,t-1} \cdot \sum_{\omega=1}^{NC} \mathbf{P}_{\omega} \cdot \left[\lambda_{2_{it\omega}} \cdot (\mathbf{GT}_i^{\min} - \mathbf{R}_i^{\text{up}}) \right] + \\
& \sum_{r=1}^{NR} \sum_{t=1}^T z_{rt} \cdot \sum_{\omega=1}^{NC} \mathbf{P}_{\omega} \cdot \left(-\beta_{1_{rt\omega}} \mathbf{C}2_r^{(d)} - \mathbf{GH}_r^{\max} \cdot \beta_{2_{rt\omega}} \right. \\
& \left. + \mathbf{GH}_r^{\min} \cdot \beta_{3_{rt\omega}} + \mathbf{GH}_r^{\max} \cdot \beta_{4_{rt\omega}} - \mathbf{GH}_r^{\min} \cdot \beta_{5_{rt\omega}} \right. \\
& \left. + \mathbf{D}1_r^{(e)} \cdot \beta_{6_{rt\omega}} + \mathbf{Q}_r^{\min} \cdot \beta_{7_{rt\omega}} - \mathbf{Q}_r^{\max} \cdot \beta_{8_{rt\omega}} \right) \geq \sum_{\omega=1}^{NC} \mathbf{P}_{\omega} \cdot \left\{ \mathbf{OF}_{\omega} \right. \\
& \left. + \sum_{i=1}^{NT} \sum_{t=1}^T \mathbf{U}_{it} \cdot \left[\lambda_{1_{it\omega}} \cdot (\mathbf{GT}_i^{\min} - \mathbf{R}_i^{\text{down}}) + \lambda_{3_{it\omega}} \cdot \mathbf{GT}_i^{\min} - \lambda_{4_{it\omega}} \cdot \mathbf{GT}_i^{\max} \right] \right. \\
& \left. + \sum_{i=1}^{NT} \sum_{t=2}^T \mathbf{U}_{i,t-1} \cdot \left[\lambda_{2_{it\omega}} \cdot (\mathbf{GT}_i^{\min} - \mathbf{R}_i^{\text{up}}) \right] + \sum_{r=1}^{NR} \sum_{t=1}^T \mathbf{Z}_{rt} \cdot \left(-\beta_{1_{rt\omega}} \mathbf{C}2_r^{(d)} \right. \right. \\
& \left. \left. - \mathbf{GH}_r^{\max} \cdot \beta_{2_{rt\omega}} + \mathbf{GH}_r^{\min} \cdot \beta_{3_{rt\omega}} + \mathbf{GH}_r^{\max} \cdot \beta_{4_{rt\omega}} - \mathbf{GH}_r^{\min} \cdot \beta_{5_{rt\omega}} \right. \right. \\
& \left. \left. + \mathbf{D}1_r^{(e)} \cdot \beta_{6_{rt\omega}} + \mathbf{Q}_r^{\min} \cdot \beta_{7_{rt\omega}} - \mathbf{Q}_r^{\max} \cdot \beta_{8_{rt\omega}} \right) \right\}
\end{aligned} \tag{4.54}$$

$$\begin{aligned}
& \theta + \sum_{i=1}^{NT} \sum_{t=1}^T u_{it} \cdot \sum_{\omega=1}^{NC} \mathbf{P}_{\omega} \cdot \left[\lambda_{1_{it\omega}} \cdot (\mathbf{GT}_i^{\min} - \mathbf{R}_i^{\text{down}}) + \right. \\
& \left. \lambda_{3_{it\omega}} \cdot \mathbf{GT}_i^{\min} - \lambda_{4_{it\omega}} \cdot \mathbf{GT}_i^{\max} \right] + \\
& \sum_{i=1}^{NT} \sum_{t=2}^T u_{i,t-1} \cdot \sum_{\omega=1}^{NC} \mathbf{P}_{\omega} \cdot \left[\lambda_{2_{it\omega}} \cdot (\mathbf{GT}_i^{\min} - \mathbf{R}_i^{\text{up}}) \right] + \\
& \geq \sum_{\omega=1}^{NC} \mathbf{P}_{\omega} \cdot \left\{ \mathbf{OF}_{\omega} + \sum_{i=1}^{NT} \sum_{t=1}^T \mathbf{U}_{it} \cdot \left[\lambda_{1_{it\omega}} \cdot (\mathbf{GT}_i^{\min} - \mathbf{R}_i^{\text{down}}) \right. \right. \\
& \left. \left. + \lambda_{3_{it\omega}} \cdot \mathbf{GT}_i^{\min} - \lambda_{4_{it\omega}} \cdot \mathbf{GT}_i^{\max} \right] \right. \\
& \left. + \sum_{i=1}^{NT} \sum_{t=2}^T \mathbf{U}_{i,t-1} \cdot \left[\lambda_{2_{it\omega}} \cdot (\mathbf{GT}_i^{\min} - \mathbf{R}_i^{\text{up}}) \right] \right\}
\end{aligned} \tag{4.55}$$

Finally, the BD algorithm presented in this section suffers from the same drawbacks as the cutting-plane method, i.e., oscillation and slow convergence, compounded with the fact that the master problem is combinatorial. To overcome this aspect, the BD approach tends to be used together with other methods to accelerate convergence. In general, there are four strategies to accelerate the method: decomposition strategies, solution procedures, solution generation and cut generation (RAHMANIANI, et al., 2017). Among the solution generation strategy, an efficient approach is to stabilize the master problem, since its instability is one of the widely recognized drawbacks of the classical BD algorithm. In this sense, this work uses an exact proximal bundle method (PB) to stabilise the master problem and decrease the number of iterations. The inclusion of the PB method in the BD algorithm is described in the next section.

4.5 Stabilized BD via Proximal Bundle Method

The PB method consists of a strategy to prospect a trust region, “penalizing” solutions out of this region. For more details of the PB method, we refer to the work of De Oliveira & Sagastizábal (2014) since it is not in the scope of this work to describe exactly this method. The algorithm showed below is proposed according to the specificities of this work.

To include the PB method in the algorithm, minor changes are needed in the BD algorithm described above. There are modifications in the structure of the master problem, since we must include one term in the objective function as shown below.

$$\begin{aligned} \min \sum_{i=1}^{NT} \sum_{t=1}^T (\mathbf{F}\mathbf{C}_i \cdot \mathbf{u}_{it} + sC_{it}) + \theta + \frac{1}{2} \mu_k \left(\sum_{i=1}^{NT} \sum_{t=1}^T \|\mathbf{u}_{it} - \mathbf{U}_{it}^{(iter)}\|^2 + \right. \\ \left. + \sum_{r=1}^{NR} \sum_{j=1}^{NG_r} \sum_{t=1}^T \|\mathbf{z}_{jrt} - \mathbf{Z}_{jrt}^{(iter)}\|^2 \right) \end{aligned} \quad (4.56)$$

The algorithm for the bundle method is described below:

1. Choose: lower bound $LB^{(0)} = -\infty$; upper bound $UB^{(0)} = \infty$, tolerance $tol > 0$; $\Delta^{(0)} = -\infty$; constant $m \in (0,1)$; feasible first-

stage point array $(\mathbf{U}_{it}^{(iter)}, \mathbf{Z}_{jrt}^{(iter)}); \mu^{(0)} \in (10^{-2}, 10^{-3})$ and set $iter = 1$.

2. Solve subproblems and use $\mathbf{OF}_{\omega}^{(iter)}, \mathbf{U}_{it}^{(iter)}, \mathbf{Z}_{jrt}^{(iter)}, \lambda_{it\omega}^{(iter)}, \dots, \lambda_{it\omega}^{(iter)}, \beta_{jrt\omega}^{(iter)}, \dots, \beta_{jrt\omega}^{(iter)}$, to build an optimality cut and obtain:

$$\mathbf{F}^{(iter)} = \sum_{i=1}^{NT} \sum_{t=1}^T (\mathbf{FC}_i \cdot \mathbf{u}_{it} + s\mathbf{C}_{it}) + \sum_{\omega=1}^{N_c} \mathbf{P}_{\omega} \mathbf{OF}_{\omega}^{(iter)}$$

$$\mu_{aux}^{(iter)} = 0.8\mu^{(iter-1)} \left(1 + \frac{UB^{(iter-1)} - \mathbf{F}^{(iter)}}{\Delta^{(iter-1)}} \right)^{-1}$$

3. If $(\mathbf{F}^{(iter)} \leq UB^{(iter-1)} - m \cdot \Delta^{(iter-1)})$, set $UB^{(iter)} = \mathbf{F}^{(iter)}$ and $\mu^{(iter)} = \max(0.6\mu^{(iter-1)}, \mu_{aux}^{(iter)})$
4. If $(\mathbf{F}^{(iter)} > UB^{(iter-1)} - m \cdot \Delta^{(iter-1)})$, set $UB^{(iter)} = UB^{(iter-1)}$ and $\mu^{(iter)} = \max(\mu^{(iter-1)}, \min(1.3\mu^{(iter-1)}, \mu_{aux}^{(iter)}, 10^8))$
5. Solve the master problem. Consider vectors $(\mathbf{U}_{it}^{(iter)}, \mathbf{Z}_{jrt}^{(iter)})$ and $MVAL$ as the solution found for the binary variables at iteration $iter$ and the value of the objective function, respectively. Do $LB^{(iter)} = MVAL$.
6. If $\left(\frac{UB^{(iter)} - LB^{(iter)}}{UB^{(iter)}} \right) \leq tol$, stop.
7. Use $\mathbf{OF}_{\omega}^{(iter)}, \mathbf{U}_{it}^{(iter)}, \mathbf{Z}_{jrt}^{(iter)}, \lambda_{it\omega}^{(iter)}, \dots, \lambda_{it\omega}^{(iter)}, \beta_{jrt\omega}^{(iter)}, \dots, \beta_{jrt\omega}^{(iter)}$, to build an optimality cut that must be included in the master problem. Set $\Delta^{(iter)} = UB^{(iter)} - LB^{(iter)}$, $iter = iter + 1$ and return to step 2.

5. COMPUTATIONAL RESULTS

This chapter presents the computational results of this work, where all tests were performed on an Intel® Core™ i7-2600 CPU 3.4 GHz, 4 GB RAM, and GUROBI 7.5 was used to solve MILP problems. Initially, the data of the electrical system is described. Next, the results associated with the deterministic HTUC results are presented for different HPF modeling. Finally, the chapter presents the results associated with a two-stage stochastic programming model for the HTUC problem. In all computation instances, we consider one-day planning horizon discretized in hourly steps.

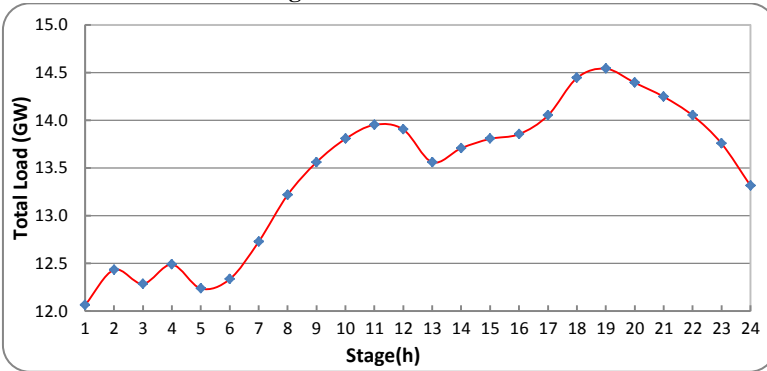
5.1 Electrical System

The hydro plants and transmission system used in this work are extracted from the Brazilian Southern power system. Thermal plants are modified from Diniz (2010), and a normal Probability Density Functions (PDFs) are assumed for the wind generation uncertainty. Specifically, the electrical system is composed of:

- 16 hydro plants, with 54 generating units; with 12,541 MW capacity
- 11 thermal plants with 3,470 MW capacity;
- Three wind farms with 1,465 MW average generation;
- A transmission system with 46 buses and 95 lines, represented as a classical DC model;
- 31 buses with load demand, where the minimum and maximum values are 10.88 and 13.36 GW, in hours 1 and 19, respectively.

Initially, Figure 5-1 shows the total load of the electrical system over the 24-hours planning horizon.

Figure 5-1 - Total load.



5.1.1 Hydro Plants

The hydro system is composed of plants located in the Iguazu and Uruguay rivers, as shown in Figure 5-2 and Figure 5-3, respectively. The plants represented by circles are run-of-the-river ones, and the triangles represent plants that have weekly or monthly regularization capacity.

Figure 5-2 – Hydro plants located in the Iguazu river.

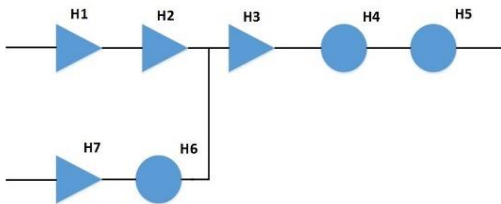
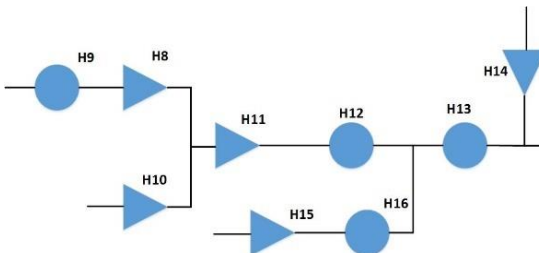


Figure 5-3 - Hydro plants located in the Uruguay River.



The water traveling time between two consecutive reservoirs is considered equals to one hour. All units in each plant are identical and possess only one forbidden operative zone. Table 5-1 shows the general

data for the hydro plants and Table 5-2 presents the minimum values for turbined outflow and power generation. We consider a 3-hours uptime and downtime constraint for all hydro units.

Table 5-1 - General data of the hydro plants.

Plant	Capacity (MW)	Maximum outflow (m ³ /s)	Maximum. volume (hm ³)	Minimum. volume (hm ³)	Units
H ₁	1,676	1,376	5,779	1,974	4
H ₂	1,260	1,268	2,950	2,562	4
H ₃	1,420	1,576	6,775	2,662	4
H ₄	1,078	1,784	1,124	721	4
H ₅	1,240	2,100	3,573	3,308	4
H ₆	120	152	35	32	2
H ₇	120	162	431	169	2
H ₈	880	558	1,477	1,320	3
H ₉	192	501	296	232	3
H ₁₀	690	516	4,904	2,712	3
H ₁₁	1,140	1,311	3340	2,283	3
H ₁₂	1,450	1,590	5100	4,300	5
H ₁₃	855	1,888	1,501.8	1,428	4
H ₁₄	120	114	137	111	3
H ₁₅	226	102	1,589	185	2
H ₁₆	74	134	150	140	2

Table 5-2 - Operation zones and productivity.

Plant	Minimum outflow (m ³ /s)	Minimum Capacity (MW)	Productivity (MW/(m ³ /s))
H ₁	688	838	1.21
H ₂	634	630	0.99
H ₃	788	710	0.90
H ₄	892	539	0.60
H ₅	1050	620	0.59
H ₆	76	60	0.79
H ₇	81	60	0.74
H ₈	279	440	1.57
H ₉	250.5	96	0.38
H ₁₀	258	345	1.33
H ₁₁	655.5	570	0.87
H ₁₂	795	725	0.91
H ₁₃	944	427.5	0.45
H ₁₄	57	60	1.05
H ₁₅	51	113	2.21
H ₁₆	67	37	0.55

Table 5-3 shows Mean Relative Error (MRE) between the linear and original nonlinear HPF and the number of constraints associated with the piecewise linear HPF models used in this work.

Table 5-3 – HPF data.

Plant	Individual (DF1-DF2-DF3)		Aggregated (DF4-DF5)	
	MRE (%)	Number of constraints	MRE (%)	Number of constraints
H ₁	0.29	8	1.95	5
H ₂	0.34	14	1.44	9
H ₃	0.20	8	1.50	5
H ₄	0.23	8	1.47	5
H ₅	0.30	8	1.46	8
H ₆	0.55	8	1.49	6
H ₇	0.29	8	2.35	4
H ₈	0.32	18	1.08	8
H ₉	0.37	14	1.78	9
H ₁₀	0.09	8	1.63	6
H ₁₁	0.24	8	1.77	6
H ₁₂	0.25	9	2.02	4
H ₁₃	0.35	8	1.27	7
H ₁₄	0.45	18	1.06	10
H ₁₅	0.41	6	3.13	8
H ₁₆	0.29	18	1.72	7

The FCF used in this work is a piecewise linear function with 250 cuts. This function involves the final volumes of all hydro plants with regulation capacity. The other ones (run-of-the-river plants) have a small storage capacity and they are not considered in the function. The FCF is obtained using the SDDP algorithm for solving a medium-term generation scheduling problem. This function is built iteratively, associating an expected cost of the water with thermal costs. More details on how this function is obtained can be seen in Tahan (2016).

Table 5-4 shows the inflow data used in the system, which were selected in order to avoid infeasibilities in the minimum power generation of the hydro units. The inflows are constant values throughout the time horizon.

Table 5-4 - Inflows.

Hydro Plant	Inflow (m ³ /s)
H ₁ / H ₂ / H ₄ / H ₁₂	350
H ₃	400
H ₅ *	1000
H ₆ */ H ₇	80
H ₈ / H ₁₀	200
H ₉ *	250
H ₁₁	450
H ₁₃ *	950

5.1.2 Thermal Plants

Table 5-5 presents the data related to the thermal plants.

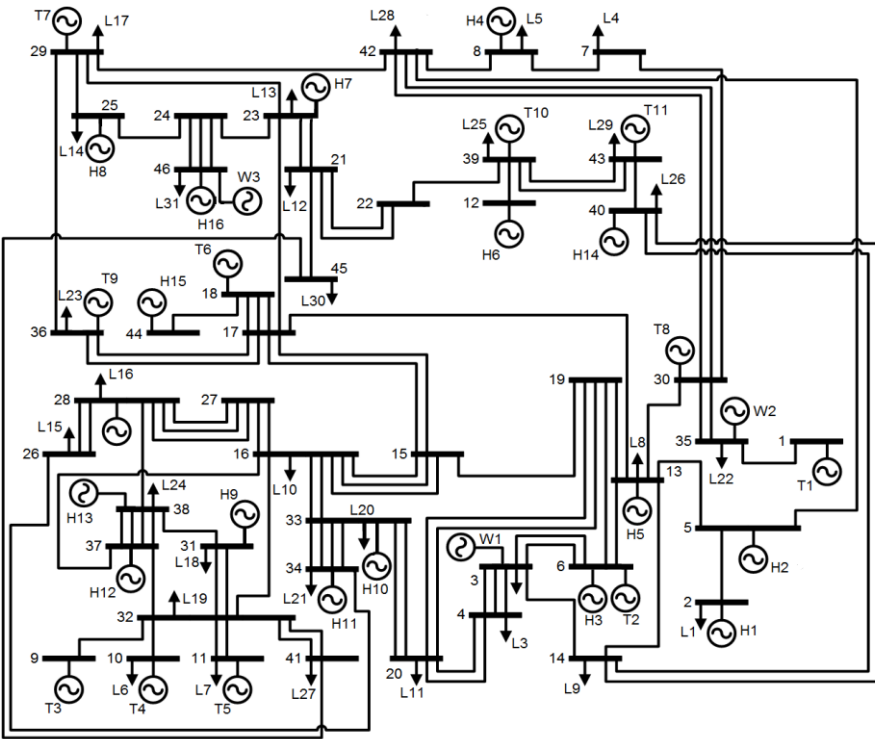
Table 5-5 - General data for thermal plants.

Plant	Fixed Cost (R\$)	Unitary variable cost (R\$/MW)	Startup cost (R\$)	Maximum power (MW)	Minimum power (MW).	Ramp (MWh/h)	Minimum up/down-time (h)
T ₁	135	13	1,300	150	30	40	8
T ₂	122	12	1,200	220	100	40	4
T ₃	110	11	1,100	155	55	30	5
T ₄	105	10	1,000	155	55	30	6
T ₅	30	9	200	350	110	60	3
T ₆	1050	10.5	10,500	350	140	30	1
T ₇	245	20	2,400	350	70	70	4
T ₈	212	21	2,100	560	200	180	8
T ₉	263	26	2,600	60	12	12	1
T ₁₀	235	20	2,300	560	200	180	8
T ₁₁	220	25	2,200	560	200	180	4

5.1.3 Transmission System

The transmission system has 46 buses and 95 lines, whose data was extracted from the Brazilian southern electrical system (SCUZZIATO, 2016). Figure 5-4 shows the transmission system, as well as the power plants and loads location. Letters L, T, W, and H represent loads, wind farms, thermal and hydro plants, respectively. Bus 34 is considered as a slack bus. The Appendix A shows the data of the transmission lines used in the classical DC model power flow (reactance, lines capacity, etc.).

Figure 5-4 - Power plants, loads, and transmission system configuration.



5.1.4 Wind Power Scenario Generation

The random variable in the stochastic HTUC model is the power generation of the wind farms. Scenario generation is a very complex issue and, since it is not the focus of this work, this issue is simplified in comparison with real-life problems. In this sense, the wind farms are modeled via the lag-one periodic autoregressive model, that is, the wind generation depends linearly on its own previous values. The equations that represent the autoregressive models used in each wind farm are given by:

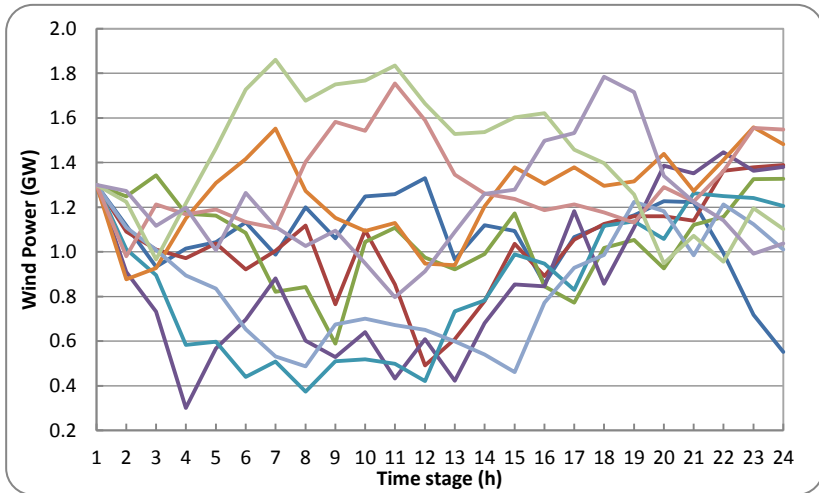
$$\begin{aligned}
 gw_{1t} &= 0.93 \cdot gw_{1,t-1} + \xi(70,150) \\
 gw_{2t} &= 0.95 \cdot gw_{2,t-1} + \xi(-5,60) \\
 gw_{3t} &= 0.10 \cdot gw_{3,t-1} + \xi(100,35)
 \end{aligned}
 \tag{4.57}$$

where:

- t index of periods (h);
 gw_{it} power generation of wind farm i and stage t (MW);
 $\xi(\mu, \sigma)$ residual of the autoregressive model represented as a normal PDF with a mean μ and standard deviation σ .

Figure 5-5 shows 10 wind scenarios that will be used ahead, where each scenario corresponds to the sum of the three wind farms generation.

Figure 5-5 – Aggregated wind generation scenarios.



5.2 Deterministic cases

This section presents results of 20 deterministic HTUC cases using the 10 wind generation scenarios combined with two initial volumes of the reservoirs (40 and 80 % useful volumes). Table 5-6 shows the initial volume of the reservoirs.

Table 5-6 - Initial volumes of hydro plants (hm³).

Plant	40%	80%
H ₁	3,496	5,018
H ₂	2,717	2,872
H ₃	4,307	5,952
H ₄	882	1,043
H ₅	3,414	3,520
H ₆	33	34
H ₇	273	377
H ₈	1,382	1,445
H ₉	257	283
H ₁₀	3,588	4,465
H ₁₁	2,705	3,128
H ₁₂	4,620	4,940
H ₁₃	1,457	1,487
H ₁₄	121	132
H ₁₅	746	1,308
H ₁₆	144	148

The deterministic analysis aims to evaluate individual and aggregated HPF models in terms of solution quality and computational time. This benchmark supports which HPF modeling will be included in the two-stage HTUC problem instances.

5.2.1 Individual Representation of the Hydro Units

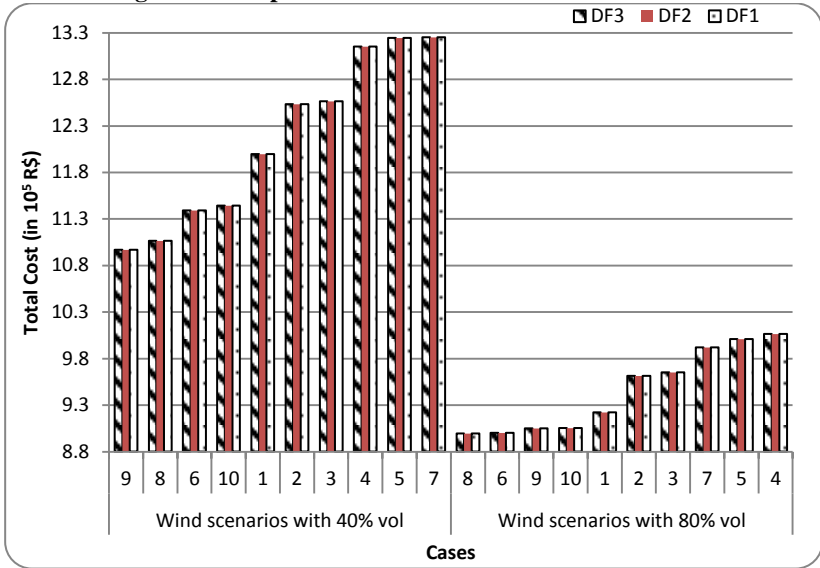
In this subsection, the HTUC problem considering different individual hydro units representation, i.e., DF1, DF2, and DF3, are evaluated. The associated MILPs have different numbers of constraints and variables, which are seen in Table 5-7.

Table 5-7 – Variables and constraints for individual HPF modeling.

HPF modeling	DF1	DF2	DF3
binary variables	1,512	1,512	1,512
continuous variables	8,161	9,073	8,161
constraints	37,142	39,638	23,075

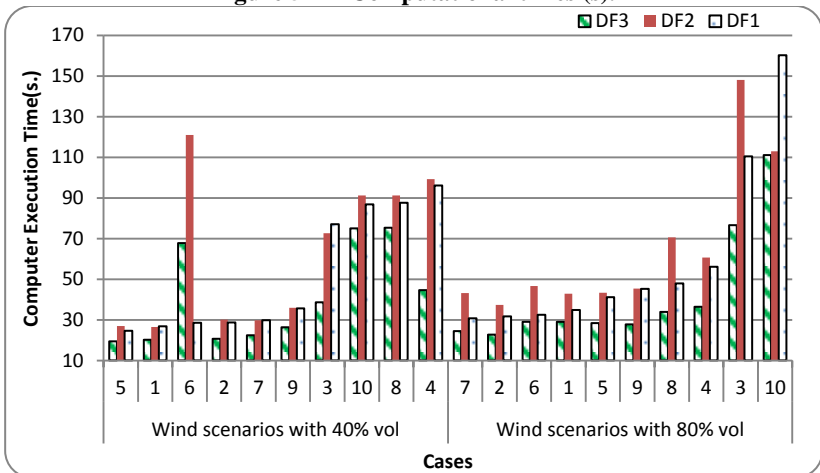
Figure 5-6 presents the optimal value of the objective function for each HPF case. All executions were performed using a standard GUROBI MIPgap, that is 0.01 %. The maximum relative difference was 0.00039% (smaller than GUROBI MIPgap and therefore negligible) and has occurred between DF1 and DF2 for wind scenario 6 using an 80% useful volume. As expected, the different HPF models do not change the optimal cost.

Figure 5-6 – Optimal costs for the deterministic MILPs.



The main issue is associated with the computational time, as presented in Figure 5-7.

Figure 5-7 – Computational times (s).



The model DF3 confirms its efficiency, except for Scenario 6 and 40% initial volume, in which optimal costs of R\$ 1,138,934.46 and R\$ 1,138,938.52 have been found in 67.8 and 28.51 seconds for models DF3 and DF1, respectively. However, when MIPgap is set equals

0.02%, GUROBI found a R\$ 1,138,932.23 optimal cost (0.0002% difference) in 22.42 seconds for model DF3. Using this same MIPgap for model DF1, it is obtained the same R\$ 1,138,938.52 optimal cost in 26.88 seconds. Thus, the computation time for this case is adjusted through GUROBI parameters, which do not jeopardize the optimal solution found. Table 5-8 shows the average cost and the respective standard deviation for the cases.

Table 5-8 – Average (\bar{x}) and standard deviation (S) of the optimal costs (R\$).

Initial Volumes (hm ³)	(R\$).			
	DF1	DF2	DF3	
40%	\bar{x}	1,215,949.41	1,215,948.82	1,215,953.35
	S	86,057.76	86,058.29	86,060.07
80%	\bar{x}	945,774.23	945,774.16	945,774.07
	S	41,808.16	41,809.2	41,808.52

Table 5-9 presents the average and standard deviation values associated with the computational times. It is seen that computational burden depends strongly on the HPF model. The greatest average difference is between models DF2 and DF3 (41.7% related to 40% volume cases).

Table 5-9 - Average and standard deviation of the computational times (s).

Initial Volumes (hm ³)	DF1	DF2	DF3	
40%	\bar{x}	52.12	62.47	36.40
	S	28.77	34.52	22.25
80%	\bar{x}	59.04	65.06	41.90
	S	42.63	36.78	28.81

Finally, we show examples of dispatch provided by DF1 and DF3. The Table 5-10 contains the turbined outflow decisions for H₅ in the Scenario 4 and 80% volume. The second table contains the same data for H₉ in Scenario 8 and 40% volume. As shown, the total turbined outflow in the plants is very similar, which has as consequence the similarity of the costs as well.

Table 5-12 and Table 5-13 show the same situation but for the power generation. This pattern of similar generation occurs for the other scenarios as well.

Table 5-10 - Turbined outflow in H₅ at stage 6 (m³/s).

		H ₅ turbined outflow				
Scenario 4 80% volume	Unit	1	2	3	4	Plant
	DF1	294.90	0	267.20	372.92	935.02
	DF3	0	311.67	311.67	311.67	935.01

Table 5-11 - Turbined outflow in H₉ at stage 9 (m³/s).

		H₉ turbined outflow			
Scenario 8	Unit	1	2	3	Plant
40% volume	DF1	162.75	170.90	171.00	504.65
	DF3	168.21	168.21	168.21	504.63

Table 5-12 - Power generation decisions in H₅ plant in stage 6 (MW).

		H₅ power generation				
Scenario 4	Unit	1	2	3	4	Plant
80% volume	DF1	167.70	0	150.70	215.55	533.95
	DF3	0	177.98	177.98	177.98	533.94

Table 5-13 - Power generation decisions in H₉ plant in stage 9 (MW).

		H₉ power generation			
Scenario 8	Unit	1	2	3	Plant
40% volume	DF1	56.12	58.84	58.85	173.81
	DF3	57.93	57.93	57.93	173.79

We see that generation and costs are very similar between DF1 and DF3, while the computational burden is significantly smaller for DF3 than for DF1. Thus, the DF3 model will be used to evaluate the performance of the aggregated models.

5.2.2 Aggregated Hydro Units

In this subsection, we are interested in the HTUC problem where the HPFs are represented according to DF4 and DF5 models. It is important to emphasize that for the model DF4, the minimum value of a hydro plant's power generation is the minimum generation of a single unit for the individual representation, and for DF5 this value is zero since there is no binary variable that can control the minimum generation. Table 5-14 shows the number of variables and constraints for DF4 and DF5 models.

Table 5-14 – Number of variables and constraints for DF4 and DF5 models.

MILP	DF4	DF5
Binary variables	648	264
Continuous variables	4,465	4,465
Constraints	10,623	10,623

The same scenarios used in the individual models were applied to the aggregated ones and Figure 5-8 presents the optimal objective function values for each scenario. It is seen that these values are very similar in comparison with DF3 model. The maximum relative error is 1.2 % obtained between DF3 and DF5, in scenario 6 and 80% initial volumes.

The minimum and average relative errors between DF3 and DF5 considering all cases are 0.59% and 0.72%, respectively.

Figure 5-8 - Total cost for the 20 Cases.

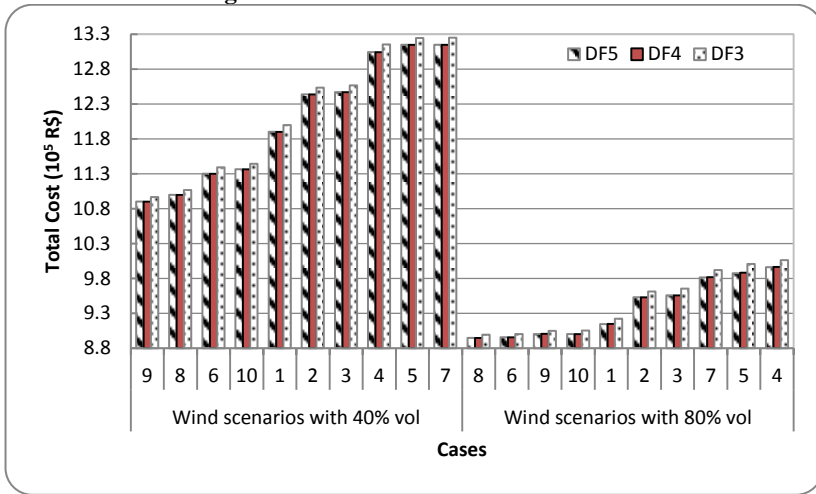


Figure 5-9 presents the computational time for all cases (including DF3 – the benchmark MILP), where the DF5 appears more efficient than DF4. In terms of computational burden, the greatest difference is verified between DF3 and DF5 for scenario 10 and 80% initial volumes. In this case the computational time of DF3 is approximately 7 times higher than for DF5. On average, the DF3 model has a computational burden 3.1 higher than DF5. The minimum difference between these models is a factor of 1.8.

Figure 5-9 - Computational Execution Time (s).

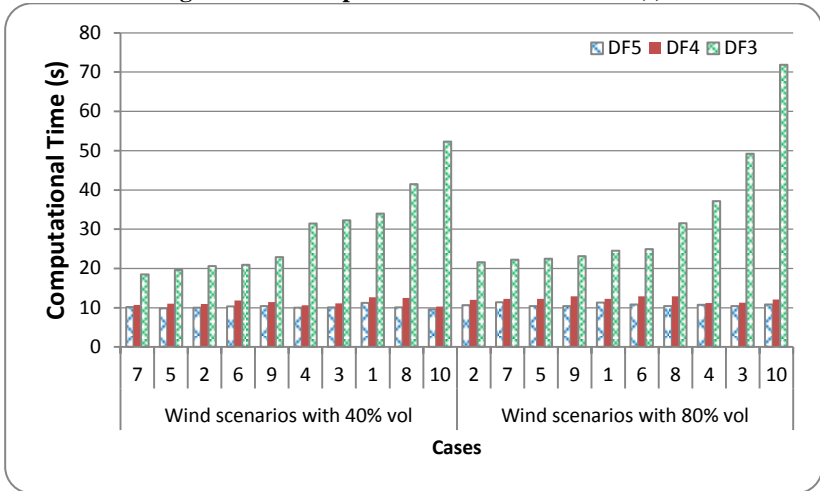


Table 5-15 and Table 5-16 include the average and standard deviation of optimal costs, as well as the computational execution time for all three MILPs. As a conclusion, we can see that, through comparison to DF3, DF5 model provides very accurate solutions with low computational effort.

Table 5-15 - Average and standard deviation of the optimal costs (R\$).

Initial Volumes (hm ³)		DF3	DF4	DF5
40%	μ	1,215,953.35	1,207,026.89	1,206,992.72
	σ	90715.28	89456.75	89418.91
80%	μ	945774.07	938314.77	937941.09
	σ	44070.05	41463.65	41214.40

Table 5-16 - Average and standard deviation of the computational time (s).

Initial Volumes (hm ³)		DF3	DF4	DF5
40%	μ	29.36	11.31	10.13
	σ	11.10	0.78	0.43
80%	μ	34.82	13.47	11.25
	σ	2.72	0.78	0.54

5.3 Stochastic Instances

In this section, we present the computational results associated with the two-stage stochastic HTUC problem. We presented in the previous

chapter stochastic models: SF1, SF2, and SF3, according to the HPF modeled. Table 5-17 shows the size of each stochastic model.

Table 5-17 - Stochastic cases for 10 scenarios.

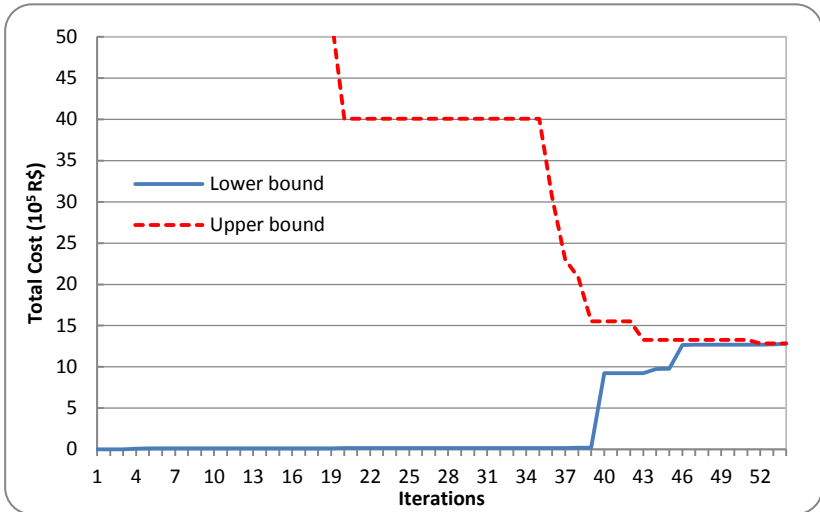
Model	SF1	SF2	SF3
Binary variables	1,512	648	264
Continuous variables	81,610	44,650	44,650
Constraints	230,750	106,230	106,230

Since SF2 and SF3 have similar formulations, in this section we analyze only SF1 and SF3. In this sense, we consider four scenario trees, each one with 10 wind generation sample size. These trees will be evaluated with 40% and 80% of useful volume as initial conditions of volume. In all BD computational instances, the algorithm finishes when the algorithm reaches 500 iterations or when $(z_{up} - z_{lo})/z_{up} \leq 0.5\%$, where z_{up} is the best upper bound and z_{lo} is the lower bound. The MILP related to the master problem in BD is solved via Gurobi with MIP gap equals to 10^{-8} . The second-stage LP subproblems are also solved with Gurobi using the same tolerance. The remaining of this section is organized as follows: initially the analyses consider the reservoirs with 40% initial volumes; next, the focus is on the cases with 80% initial volumes.

5.3.1 Reservoirs with 40% Initial Volumes

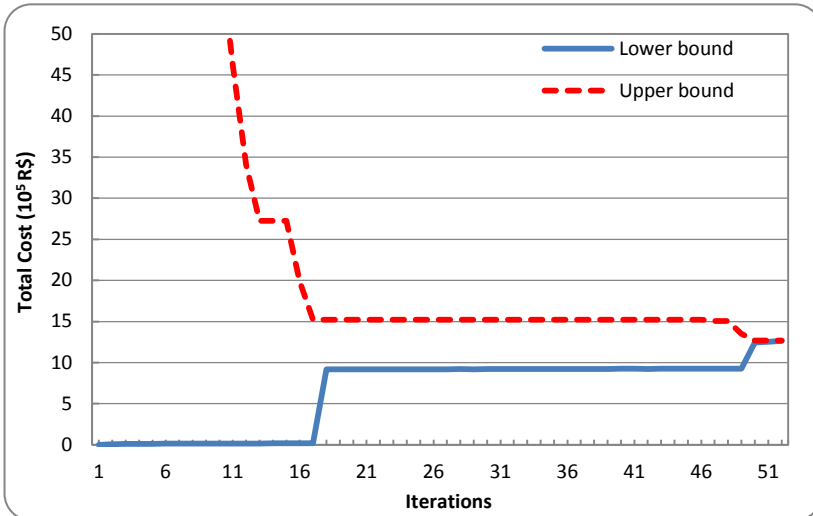
Initially, we consider the 10 scenarios shown in Figure 5-5. Figure 5-10 depicts the values of lower and upper bounds over the iterative process for model SF1.

Figure 5-10 - Lower and Upper bounds for SF1 case.



As shown above, the algorithm has converged in 54 iterations, where Z_{up} is R\$1,259,722.39 and Z_{lo} is R\$1,257,832.8. This computational instance took 659.78 seconds to achieve convergence. On the other hand, Figure 5-11 depicts the convergence process for model SF3. In this case, the algorithm needed 52 iterations for attending the stopping criteria, resulting in a Z_{up} of R\$ 1,252,459.12 and Z_{lo} of R\$1,251,056.36. Its computational time was 301.53 seconds.

Figure 5-11 - Lower and upper bounds for SF3 case.



Based on these computational instances, the relative difference between SF3 and SF1 for Z_{up} is 0.57%. On the other hand, the difference verified in the execution time is substantial, since SF1 demands approximately 2.2 times more computational effort than SF3 to converge.

5.3.2 Reservoirs with 80% Initial Volumes

The cases with 80% of initial volumes have lower costs when compared to the 40% cases. However, in such cases there are more candidates to the optimal solution, especially among the hydro generation, i.e., it is possible to generate the same power with a greater number of combinations of hydro units.

Figure 5-12 and Figure 5-13 show lower and upper bounds for models SF1 and SF3, respectively. For SF1, the BD reached convergence in 56 iterations in 885.81 s. In the last iteration, the Z_{up} is R\$ 983,618.08, Z_{lo} is R\$ 983,500.04 and consequently, the BD optimality gap is 0.012%. On the other hand, model SF3 converged in 48 iterations with a 281.59 (s) computational time. In this case, Z_{up} is R\$ 963,744.15, Z_{lo} is R\$ 965,256.67 and the optimality gap is 0.36%. The difference between Z_{up} for the models is 2%, and SF1 has a computational burden 3.14 higher than SF3.

Figure 5-12 - Lower and upper bounds for SF1 case (80% vol)

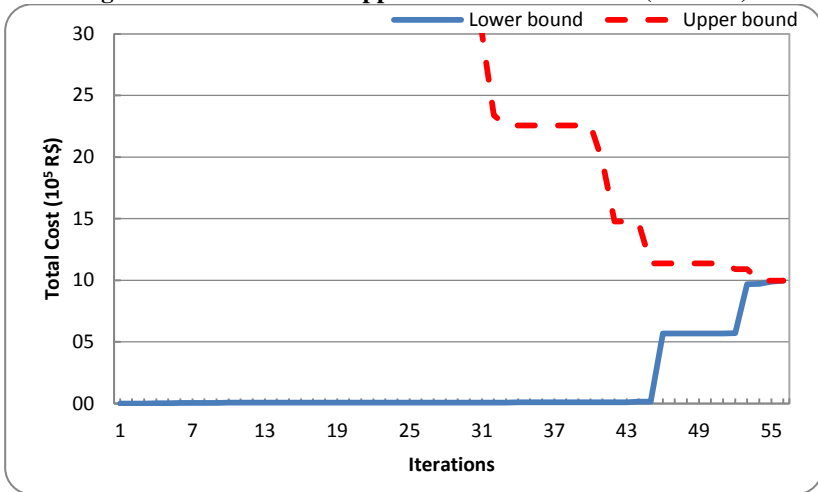
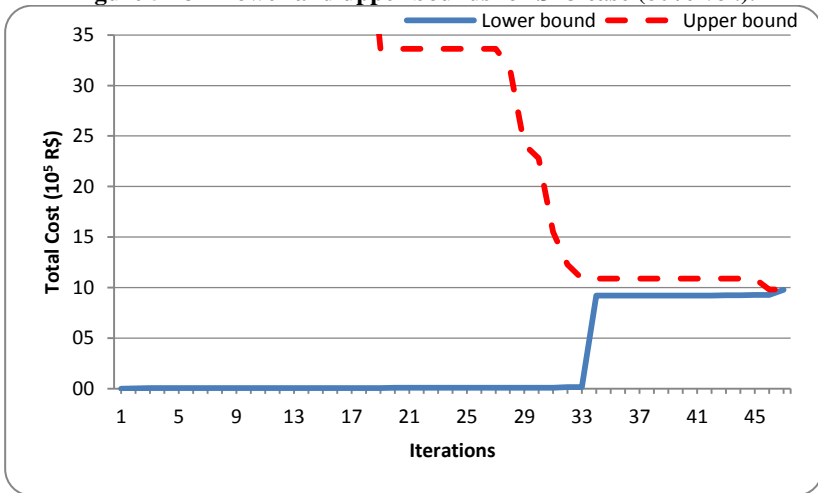


Figure 5-13 - Lower and upper bounds for SF3 case (80% vol.).



5.3.3 Additional Computational Instances

Besides the instances presented, the algorithm was also executed considering other 3 trees with 10 wind generation scenarios each. The averages and standard deviations of the trees in each hour are shown in the figures below, including the tree used in the previous cases.

Figure 5-14 – Mean (left axis) and the standard deviation for Tree 1.

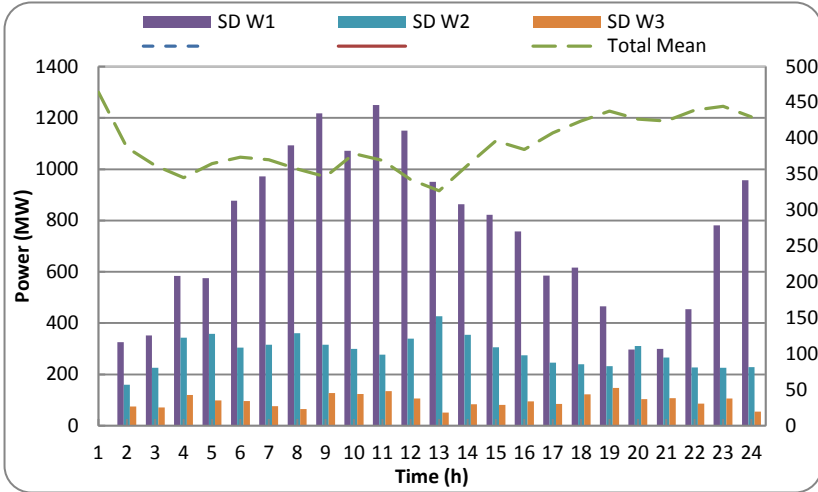


Figure 5-15 – Mean (left axis) and the standard deviation for Tree 2.

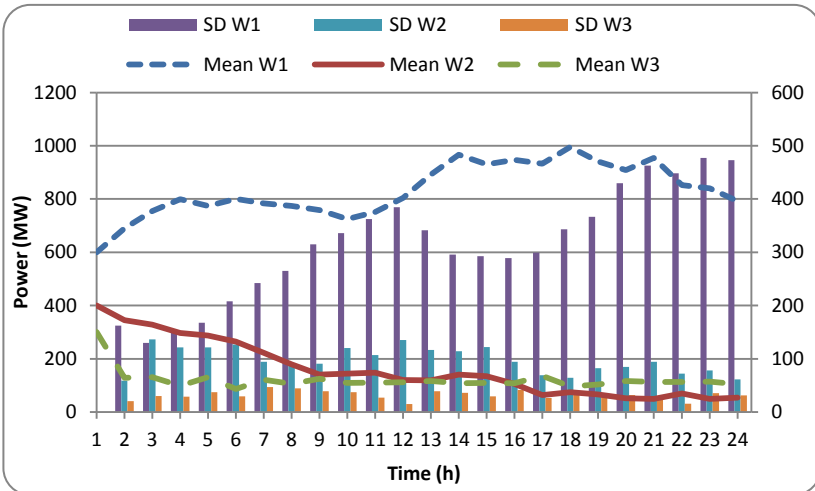


Figure 5-16 – Mean (left axis) and the standard deviation for Tree 3.

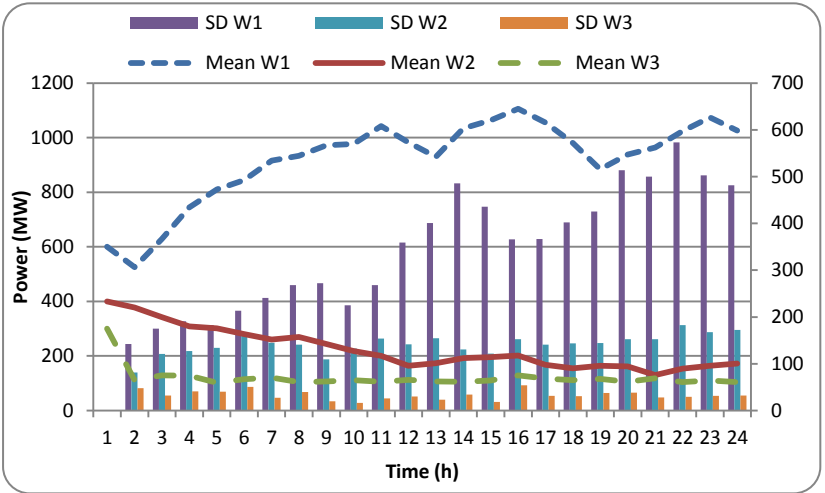
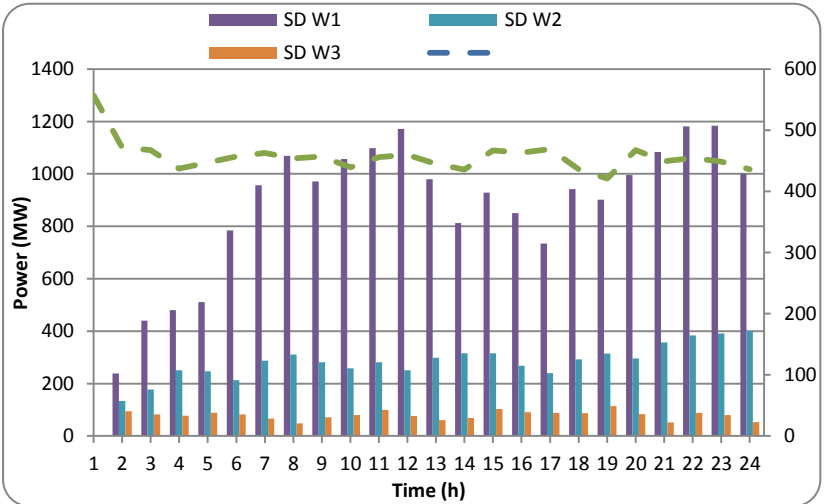


Figure 5-17 - Mean (left axis) and the standard deviation for Tree 4.



The tables presented ahead summarize the main results for the SF1 and SF3 HTUC problems, considering all trees and initial volumes.

Table 5-18 - Stochastic cases for model SF1 (40% vol).

Case	It.	Time (min.)	Zsup (R\$ x 10 ⁶)	Immediate Cost (R\$ x 10 ⁶)	Future Cost (R\$ x 10 ⁶)	Thermal Generation (TWh)	Hydro Generation (TWh)
1	54	10.99	1.259	0.368	0.891	15.238	252.971
2	52	13.70	1.303	0.411	0.891	15.387	252.338
3	54	11.18	1.225	0.335	0.890	12.891	251.221
4	97	17.99	1.340	0.449	0.890	16.681	252.195

Table 5-19 - Stochastic cases for model SF3 (40% vol)

Case	It.	Time (min.)	Zsup (R\$ x 10 ⁶)	Immediate Cost (R\$ x 10 ⁶)	Future Cost (R\$ x 10 ⁶)	Thermal Generation (TWh)	Hydro Generation (TWh)
5	52	5.02	1.252	0.361	0.891	14.906	253.303
6	57	4.96	1.295	0.404	0.891	14.736	252.989
7	50	4.6	1.221	0.330	0.890	12.794	251.318
8	80	6.28	1.324	0.433	0.890	16.177	252.699

Table 5-20 - Stochastic Cases for model SF1 (80% vol).

Case	It.	Time (min.)	Zsup (R\$ x 10 ⁶)	Immediate Cost (R\$ x 10 ⁶)	Future Cost (R\$ x 10 ⁶)	Thermal Generation (TWh)	Hydro Generation (TWh)
9	56	14.76	0.983	0.163	0.820	7.139	261.070
10	89	11.65	1.058	0.239	0.819	8.734	258.992
11	110	15.34	0.988	0.169	0.819	6.620	257.492
12	61	11.12	1.069	0.249	0.819	10.129	258.746

Table 5-21 - Stochastic Cases for model SF3 (80% vol)

Case	It.	Time (min.)	Zsup (R\$ x 10 ⁶)	Immediate Cost (R\$ x 10 ⁶)	Future Cost (R\$ x 10 ⁶)	Thermal Generation (TWh)	Hydro Generation (TWh)
13	48	4.69	0.968	0.148	0.820	6.692	261.517
14	70	6.87	1.042	0.223	0.819	8.329	259.396
15	111	6.33	0.977	0.158	0.819	6.328	257.784
16	83	8.17	1.051	0.231	0.820	9.309	259.567

We can see that, in all cases, the SF3 costs are lower than SF1 ones. Highest and lowest differences between the Z_{up} are 1.69% (between cases 12 and 16) and 0.34% (between cases 3 and 7). Mean error for Z_{up} in 40% cases is 0.67% and for 80% is 1.47%. The highest difference between computational execution time is related to the cases 9 and 13, in which SF1 has a computation burden 3.14 times higher than SF3. For the 40% cases, the SF1 model has a computational time of 2.5 (mean) higher than SF3, and this factor for the 80% cases is 2.15. The lowest burden difference is between cases 16 and 12. In terms of thermal generation, for the 40% cases we obtained a mean difference of 2.54% and 5.85% for the 80% cases. For the hydro generation, these differences are 0.15% and 0.18% for 40% and 80% cases, respectively.

6. CONCLUDING REMARKS

In this work, we have described the HTUC as a mathematical optimization problem that seeks to minimize costs of supplying energy to a load during a 24-hours planning horizon. The HTUC, when applied to large-scale systems, may have difficult issues to converge due to the integer nature of the problem. In this sense, one of the major difficulties is related to the hydropower production, which in this work is represented using different piecewise linear functions. This representation is broadly used in the literature, but for hydro predominant systems, it may be demanding in terms of computational effort due to the many constraints associated with the piecewise model. To minimize this issue, an approach with aggregated hydro units is proposed and compared to the individual representation.

Initially, a deterministic analysis is performed using the GUROBI solver to solve a MILP problem for 10 scenarios composed of two different initial volumes. Firstly, DF3 (individual model with aggregated constraints) is compared with DF1 (individual model with individual constraints), and it was seen that the hydro generation in DF1 is very similar to DF3, which led to a similarity of the optimal costs as well. The average difference between these two models is negligible, while the computational burden for DF1 is about 30% higher. After that, the DF3 and DF5 (aggregated model without binary variables for hydro plants) models are compared. The mean relative error of optimal costs between these ones is 0.72%. On the other hand, the average computational time is significantly smaller for the aggregated model, where for DF3 it is 32.09 s. while for DF5 is 10.69 s.

The comparison among the individual models (DF1, DF2 and DF3) show that the approach of aggregating constraints (DF3 model) increases the efficiency to solve the HTUC problem, since we reach the same results of costs and generation of the complete individual model (DF1) with less computational burden. Moreover, the comparison between DF3 and the aggregated model DF5 demonstrates that the difference between the individual and aggregated models is very small, even though for real-life instances the aggregated approach may provide impractical decisions since the operation zones of the hydro units are altered. However, since the difference between the models is not great, it is perfectly reasonable to use the DF5 model to obtain preliminary results regarding costs and generation. Furthermore, for very large scale systems, DF5 models may be a practical solution for real operation,

since in some cases DF1 or DF3 may not even reach convergence to the dimension of the problem

Next, a stochastic analysis is performed for the same tree with 10 scenarios used in the deterministic analysis. Furthermore, we have used other 3 trees with 10 scenarios, totalizing 4 trees. The two stochastic models SF1 (individual model with aggregated constraints) and SF3 (aggregated model without binary variables for hydro units) are compared and the results show minor differences associated with the optimal costs, but reasonable distinctions regarding the computation burden. In general, the greatest differences have been noticed for cases with 80% initial volumes. The relative difference in the optimal costs between SF1 and SF3 is approximately 1% for all the cases. In terms of total generation, the greatest difference was noticed for the thermal dispatch: mean of 4.5% for all the cases.

The same analysis of the deterministic cases is applied for the stochastic instances, i.e., even though the SF3 model alters the real operation zones of the hydro units, it provides solid results in terms of costs and generation proven by the similar results compared to the SF1 model, and then can be used as preliminary results or even practical solutions in the HTUC problem depending on the dimension of the system.

6.1 Suggestions for future works

The following aspects are suggested as future developments:

- The inclusion of other random variables mainly forecasted demand and inflow, which are important factors for the model accuracy and would increase the difficulty of convergence.
- Use of a multi-stage model. Considering the inclusion of more random variables, the model becomes more stochastic and may need to be divided into more stages so that each stage would carry a reasonable amount of randomness.
- Explore other techniques to make BD decomposition more stable and include more realistic scenarios in the tree.
- Consider not only identical units in the aggregated model and evaluate this modification in terms of costs and computational burden;
- Apply the algorithm for the Brazilian system, which has 219 hydro plants with 1,267 generating units and 2,952 thermal plants (ANEEL, 2017).

7. APPENDIX A: TRANSMISSION LINES CAPACITY

T.L	Bus (origin)	Bus (end)	React. (pu)	Flow Capacity (MW)	T.L	Bus (origin)	Bus (end)	React. (pu)	Flow Capacity (MW)
TL1	3	4	0,0161	800	TL49	23	21	0,0276	500
TL2	3	4	0,0161	800	TL50	23	21	0,0276	672
TL3	3	4	0,017	900	TL51	24	25	0,0034	400
TL4	3	6	0,0121	750	TL52	26	28	0,0297	280
TL5	3	6	0,0126	750	TL53	26	28	0,0297	150
TL6	4	20	0,0182	724	TL54	26	34	0,1872	545
TL7	4	20	0,0262	724	TL55	28	27	0,0601	100
TL8	5	2	0,0105	2500	TL56	28	27	0,0601	100
TL9	6	19	0,0044	2110	TL57	28	27	0,0601	100
TL10	7	8	0,0074	1637	TL58	28	38	0,2763	600
TL11	7	30	0,0243	2273	TL59	29	25	0,0355	400
TL12	13	5	0,0065	2363	TL60	29	36	0,0092	300
TL13	13	6	0,0255	2110	TL61	29	42	0,0217	1300
TL14	13	17	0,0205	2363	TL62	30	35	0,0139	1100
TL15	13	19	0,0269	2182	TL63	30	35	0,0145	1200
TL16	13	30	0,0201	2162	TL64	30	42	0,0194	300
TL17	14	3	0,2826	750	TL65	30	42	0,0201	500
TL18	14	13	0,0121	1000	TL66	31	32	0,1183	400
TL19	14	40	0,1574	600	TL67	31	32	0,1183	600
TL20	14	40	0,1572	600	TL68	31	38	0,2683	700
TL21	15	17	0,0292	2037	TL69	32	9	0,1286	159
TL22	15	19	0,016	2110	TL70	32	10	0,0449	1000
TL23	16	15	0,0115	672	TL71	32	11	0,0744	1500
TL24	16	15	0,0116	672	TL72	32	11	0,0741	130
TL25	16	15	0,0128	672	TL73	32	37	0,1188	700
TL26	16	27	0,0328	1000	TL74	32	41	0,0484	400
TL27	16	27	0,0328	650	TL75	32	41	0,0464	400
TL28	16	32	0,1936	593	TL76	34	33	0,1048	400
TL29	16	33	0,0656	693	TL77	34	33	0,0585	350
TL30	16	33	0,0656	443	TL78	34	33	0,0578	350
TL31	16	37	0,1313	446	TL79	34	33	0,1272	525
TL32	17	15	0,0391	2037	TL80	35	1	0,0141	1500
TL33	17	23	0,0235	600	TL81	36	17	0,0046	400
TL34	17	36	0,0059	420	TL82	38	37	0,1181	400
TL35	18	17	0,0124	1500	TL83	38	37	0,131	400
TL36	18	17	0,0123	1600	TL84	38	37	0,1263	500
TL37	18	17	0,0123	400	TL85	38	37	0,0598	600
TL38	18	44	0,0206	450	TL86	39	12	0,0461	291
TL39	20	19	0,0116	320	TL87	39	43	0,0778	559
TL40	20	19	0,0117	550	TL88	39	43	0,0777	559
TL41	20	33	0,0978	550	TL89	40	43	0,1589	700
TL42	20	33	0,097	550	TL90	42	5	0,007	1500
TL43	21	22	0,0304	600	TL91	42	8	0,0117	500
TL44	21	22	0,0304	600	TL92	45	41	0,1195	600
TL45	21	45	0,0818	500	TL93	46	24	0,0122	1500
TL46	22	39	0,2076	600	TL94	46	24	0,0114	1600
TL47	23	24	0,0092	1688	TL95	46	24	0,0122	1600
TL48	23	29	0,0303	2182					

8. REFERENCES

- ANDREW, A. M., 1979. Another efficient algorithm for convex hulls in two dimensions. *Information Processing Letters*, 9(5), pp. 216-219.
- ANEEL, 2017. *Capacidade de Geração do Brasil*. [Online]
Available at:
<http://www2.aneel.gov.br/aplicacoes/capacidadebrasil/capacidadebrasil.cfm>
[Accessed 15 September 2017].
- ARVANITTDIS, N. V. & ROSING, J., 1970. Composite Representation of a Multireservoir Hydroelectric Power System. *IEEE Transactions on Power Apparatus and Systems*, PAS-89(2), pp. 319-326.
- BAZARAA, M. S., SHERALI, H. D. & SHETTY, C. M., 2006. *Nonlinear Programming: Theory and Algorithms*. s.l.:Wiley-Interscience.
- BENDERS, J. F., 1962. Partitioning Procedures for Solving Mixed-variables Programming Problems. *Numerische Mathematik*, pp. 238-252.
- BEN-TAL, A. & NEMIROVSKI, A. . A. N., 2000. Robust solutions of Linear Programming problems. *Mathematical Programming*, p. 13.
- BEN-TAL, A. & NEMIROVSKI, A., 2009. On safe Tractable Approximations of Chance-Constrained Linear Matrix Inequalities. *Mathematics of Operations Research*, pp. 1-25.
- Bertsekas, D. P., 1999. *Nonlinear Programming: 3rd Edition*. 2 ed. s.l.:Athena Scientific.
- BIRGE, J. R. & LOUVEAUX, F., 2011. *Introduction to Stochastic Programming*. 2a ed. s.l.:s.n.
- BONNANS, J. F., GILBERT, J. C., LEMARECHAL, C. & SAGASTIZABAL, C. A., 2006. *Numerical Optimization*. s.l.:Springer.
- BOSCH, P. P. J. V. D., 1985. A solution of the Unit commitment via decomposition and dynamic programming. *IEEE Transactions on Power Apparatus and Systems*, Volume PAS-104, pp. 1684 - 1690.
- BOYD, S. & VANDENBERGHE, L., 2003. *Convex Optimization*. s.l.:Cambridge University Press.

BOYD, S., XIAO, L. & MUTAPIC, A., 2003. *Notes on Decomposition Methods*. s.l.:Stanford University.

BRITO, F. M., 2013. *Faraday: Um sistema de suporte à manipulação de dados do Setor Elétrico Brasileiro*. Master's thesis. Federal University of Goiás. Goiânia(GO): s.n.

CARDOZO, C., 2014. *Unit Commitment with Uncertainties - State of the art*. [Online]
Available at: <https://hal.archives-ouvertes.fr/hal-01083932/document>
[Accessed 07 June 2018].

Carpentier, P., Cohen, G. & Culioli, J. C., 1996. Stochastic Optimization of Unit Commitment: A New Decomposition Framework. *IEEE Transactions on Power Systems*, 11(2), pp. 1067-1073.

Carvalho, L. C. X. d., 2002. *Planejamento de Sistemas Hidrotérmicos: Uma Análise Comparativa entre as Representações a Usinas Individualizadas e a Reservatórios Equivalentes de Energia*. Florianópolis(Santa Catarina): Federal University of Santa Catarina.

CHANG, C. & WRIGHT, J. G., 1999. A Mixed Integer Linear Programming Based Hydro Unit Commitment. *IEEE Power Engineering Society Summer Meeting*, pp. 924-928.

CHENG, C.-P., LIU, C.-w. & LIU, C.-c., 2000. Unit commitment by Lagrangian relaxation and genetic algorithms. *IEEE Transactions on Power Systems*, 15(2), pp. 707-714.

COHEN, A. & YOSHIMURA, M., 1983. A Branch-and-Bound Algorithm for Unit Commitment. *IEEE Transactions on Power Apparatus and Systems*, PAS-102(2), pp. 444-451.

Conejo, A. J., Arroyo, J. M., Contreras, J. & Villamor, F. A., n.d. Self-scheduling of a hydro producer in a pool-based electricity market. *IEEE Transactions on Power Systems*.

COSTA, A. M., CORDEAU, J. F., GENDRON, B. & LAPORTE, G., 2012. Accelerating benders decomposition with heuristic master problem solutions. *Pesquisa Operacional*, March.

Cunha, S. H. F., Prado, S. & Da Costa, J. P., 1997. *Modelagem da Produtividade Variável de Usinas Hidroelétricas com Base na Construção de*

Uma Função de Produção Energética. s.l.:XII Simpósio Brasileiro de Recursos Hídricos.

DANTZIG, G. B. & WOLFE, P., 1960. *Decomposition principle for linear programs*. s.l.:s.n.

DE OLIVEIRA, W. & SAGASTIZÁBAL, C., 2014. Level Bundle Methods for Oracles with on-demand accuracy. *Optimization Methods & Software*, 29(6), p. 26.

DENTCHEVA, D., 2009. *Optimisation Models with Probabilistic Constraints*. In: Philadelphia: s.n.

Ding, X., Lee, W.-J., Jianxue, W. & Liu, L., 2010. Studies on Stochastic Unit Commitment Formulation with Flexible Generating Units. *Electric Power Systems Research*, Issue 130-141.

DINIZ, A. L., 2010. *Test Cases for Unit Commitment and Hydrothermal Scheduling Problems*. s.l., s.n., p. 11.

Diniz, A. L. & Piñeiro Maceira, M. E., 2008. A four-dimensional model of hydro generation for the short-term hydrothermal dispatch problem considering head and spillage effects. *IEEE Transactions on Power Systems*, 23(3), pp. 1298-1308.

ANEEL, 2017. *Informações gerenciais*. [Online]

Available at:

<http://www.aneel.gov.br/documents/656877/14854008/Boletim+de+Informa%C3%A7%C3%B5es+Gerenciais+1%C2%BA+trimestre+de+2017/798691d2-990b-3b36-1833-c3e8c9861c21>

[Accessed 29 July 2018].

EPE, 2016. *The Brazilian Commitment to Combating Climate Change: Energy Production and Use*, s.l.: s.n.

FINARDI, E. C., 2003. *Alocação de Unidades Geradoras Hidrelétricas em Sistemas Hidrotérmicos Utilizando Relaxação Lagrangeana e Programação Quadrática Sequencial*. Florianópolis: s.n.

FLOUDAS, C. A., AGGARWAL, A. & CIRIC, A. R., 1989. Global Optimum Search for Nonconvex NLP and MINLP Problems. *Computers & Chemical Engineering* 13, pp. 1117 - 1132.

- FRANGIONI, A., GENTILE, C. & LACALANDRA, F., 2009. Tighter approximated MILP formulations for unit commitment problems. *IEEE Transactions on Power Systems*, pp. 105-113.
- FREDO, G. L. M., 2016. *Análise de Diferentes Representações da Função de Produção Hidrelétrica no Problema de Planejamento da Operação Energética de Médio Prazo*. Florianópolis: s.n.
- GEOFFRION, A., 1962. Generalized Benders Decomposition. *Journal of optimization theory and applications*, pp. 237-260.
- Gil, E., Bustos, J. & Rudnick, H., 2003. Short-term hydrothermal generation scheduling model using a genetic algorithm. *Power Systems, IEEE Transactions on*, 18(4), pp. 1256-1264.
- GOVARDHAN, M., 2016. Solution to Unit Commitment with Priority. *International Journal of Advanced Research in Electrical*, 5(2), pp. 5114-5121.
- Guedes, L. S. et al., 2017. A Unit Commitment Algorithm and a Compact MILP Model for Short-Term Hydro-Power Generation Scheduling. *IEEE Transactions on Power Systems*, 32(5), pp. 3381-3390.
- GWEC, 2015. *GLOBAL WIND REPORT*, s.l.: s.n.
- HARA, K., KIMURA, M. & HONDA, N., 1966. A Method for Planning Economic Unit Commitment and Maintenance of Thermal Power Systems. *IEEE Transactions on Power Apparatus and Systems*, Volume PAS-85, pp. 427-436.
- HILLIER, F. S., 2008. *Linear and Nonlinear Programming*. s.l.:Springer.
- INFANGER, G., 1994. *Planning under uncertainty - solving large-scale stochastic linear programs*. s.l.:s.n.
- IZMAILOV, A. & SOLODOV, M., 2007. *Otimização, volume 2: Métodos computacionais*. Rio de Janeiro: Instituto de Matemática Pura e Aplicada.
- Jiang, R., Zhang, M., Li, G. & Guan, Y., 2010. Two-stage robust power grid optimization problem. pp. 1-34.
- KAUR BAWA, K. & KAUR, A., 2013. Unit Commitment by an Improved Priority List Method. *International Journal of Science and Research (IJSR) ISSN*, 14(5).

- LEE, F., 1988. Short-term thermal unit commitment-a new method. *IEEE Transactions on Power Systems*, 3(2), pp. 421-428.
- LIAHAGEN, L. & ROD, H. H., 2016. *A Distributed Algorithm for Large-scale Stochastic Optimization Problems*. s.l.:Norwegian University of Science and Technology (NTNU).
- Liahagen, L. & ROD, H. H., 2016. *A Distributed Algorithm for Large-scale Stochastic Optimization Problems Lars Liahagen*. s.l.:s.n.
- LI, X., 2013. Parallel Nonconvex Generalized Benders Decomposition for Natural Gas Production Network Planning Under Uncertainty. *Computers & Chemical Engineering*, pp. 55:97-108.
- Li, X. et al., 2014. Hydro unit commitment via mixed integer linear programming: A case study of the three gorges project, China. *IEEE Transactions on Power Systems*, 29(3), pp. 1232-1241.
- LI, X., TOMASGARD, A. & BARTON, P. I., 2012. Nonconvex Generalized Benders Decomposition for Stochastic Separable Mixed-integer Nonlinear Programs. *Journal of Optimization Theory*, pp. 424-454.
- MARTINS, L. S. A. & SOARES, S., 2014. *Insights on short-term hydropower scheduling: on the representation of water continuity equations*. Genoa, IEEE, p. 6.
- MCDANIEL, D. & DEVINE, M., 1977. A modified Benders Partitioning Algorithm for Mixed Integer Programming. *Management Science*, pp. 312-319.
- MELO, M., GAMA, F. S. D. & SILVA, M., 2005. A primal decomposition scheme for a dynamic capacitated phase-in/phase-out location problem.
- MUCKSTADT, J. A. & WILSON, R. C., 1968. An Application of Mixed-Integer Programming Duality to Scheduling Thermal Generating Systems. *IEEE Transactions on Power Apparatus and Systems*, PAS-87(12), pp. 1968-1978.
- MUKHERJEE, S. & ADRIAN, E. C., 1989. Implementation of a lagrangian relaxation based unit commitment problem. *IEEE Transactions on Power Systems*, 4(4), pp. 1373-1380.
- NIELSEN, S. S. & ZENIOS, S. A., 1997. Scalable parallel Benders Decomposition for Stochastic Linear programming, *Parallel Computing*. pp. 1069-1088.

NORBIATO, T., DINIZ, A. & BORGES, C., 2014. *A Decomposition Scheme for Short Term Hydrothermal Scheduling Problems suitable for Parallel Processing*. Wroclaw, IEEE.

ONS, 2008. *Submódulo 18.2 – Relação dos Sistemas e Modelos Computacionais*. s.l.:s.n.

ONS, 2016. *Sub.módulo 8.1 - Programação Diária da Operação Eletroenergética*. s.l.:s.n.

ONS, 2017. *SOBRE O ONS - ATUAÇÃO*. [Online]
Available at: <http://ons.org.br/pt/paginas/sobre-o-ons/atuacao>
[Accessed 15 SEPTEMBER 2017].

OUYANG, Z. & SHAHIDEHPOUR, S., 1991. AN INTELLIGENT DYNAMIC PROGRAMMING FOR UNIT COMMITMENT APPLICATION. *Transactions on Power Systems*, Volume 6, p. 7.

OZTURK, U., MAZUMDAR, M. & NORMAN, B., 2004. A Solution to the Stochastic Unit Commitment Problem Using Chance Constrained Programming. *IEEE Transactions on Power Systems*, 19(3), pp. 1589-1598.

PANG, C. K. & CHEN, H. C., 1976. Optimal short-term thermal unit commitment. *IEEE Transactions on Power Apparatus and Systems*, Volume 95, pp. 1336-1346.

PAREDES, M., MARTINS, L. S. A. & SOARES, S., 2015. Using Semidefinite Relaxation to Solve the Day-Ahead Hydro Unit Commitment Problem. *IEEE TRANSACTIONS ON POWER SYSTEMS*, Volume 30, pp. 2695-2706.

PEREIRA, M. V. F., 1989. Optimal Stochastic Operations Scheduling of Large Hydroelectric Systems. *International Journal of Electrical Power & Energy Systems*, pp. 161-169.

PETERSON, W. L. & BRAMMER, S. R., 1995. A Capacity Based Lagrangian Relaxation Unit Commitment with Ramp Rate Constraints. *IEEE Transactions on Power Systems*, 10(2), pp. 1077-1084.

PORTAL BRASIL, 2016. *BRASIL ESTARÁ ENTRE OS 20 PAÍSES COM MAIOR GERAÇÃO SOLAR EM 2018*. [Online]
Available at: <http://www.brasil.gov.br/infraestrutura/2016/01/brasil-estara-entre-os-20-paises-com-maior-geracao-solar-em-2018>
[Accessed 18 SEPTEMBER 2017].

- RAHMANIANI, R., CRAINIC, T. G., GENDREAU, M. & REI, W., 2017. The Benders Decomposition Algorithm: A literature Review. *European Journal of Operational Research*, pp. 801-817.
- SAHARIDIS, G. K. D., MINOUX, M. & LERAPETRITOU, M. G., 2009. Accelerating Benders method using covering cut bundle generation. *International Transactions in Operational Research*, 3 June.
- SALAM, S., 2007. Unit Commitment Solution Methods. *International Journal of Energy and Power Engineering*, 1(1).
- Saric, A. T. & Stankovic, A. M., 2007. Finitely Adaptive Linear Programming in Robust Power System Optimization. *Power Tech, IEEE Lausanne*, pp. 1302-1307.
- SCUZZIATO, M. R., 2016. *Modelo de Otimização Estocástica de dois Estágios para o problema da Programação Diária da Operação Eletroenergética*. UFSC, Florianópolis: s.n. Phd Thesis.
- SHAFIEE, S., ZAREIPOUR, H. H. Z. & KNIGHT, A. M., 2017. Developing Bidding and Offering Curves of a Price-Maker Energy Storage Facility Based on Robust Optimization. *IEEE Journals & Magazines*, p. 11.
- SHAHIDEPOUR, S., MA, H. & MARWALI, M., 1997. TRANSMISSION CONSTRAINED UNIT COMMITMENT BASED ON BENDERS DECOMPOSITION. *Proceedings of the American Control Conference*, p. 5.
- SNYDER, W. L., POWELLI, H. D. & RAYBURN, J. C., 1987. Dynamic programming approach to unit commitment. *IEEE Transactions on Power Systems*, 2(2), pp. 339-348.
- TAHANAN, M., ACKOOIJ, W. V., FRANGIONI, A. & LACALANDRA, F., 2018. Large-scale Unit Commitment under uncertainty: a literature survey.
- TAHAN, C. R. V., 2017. *Aplicação da Análise de Componentes Principais no Problema do Planejamento da Operação Energética de Médio Prazo*. Florianópolis: s.n.
- Takigawa, F. Y. K., 2010. *Desenvolvimento de um Modelo Computacional para o Problema da Programação Diária da Operação de Sistemas Hidrotérmicos*. Florianópolis(Santa Catarina): Federal University of Santa Catarina. Phd Thesis.
- Tavlaridis-Gyparakis, K., 2017. *Decomposition Techniques for Large-Scale Energy Optimization Problems*. s.l.:s.n.

TSENG, C.-L. e. a., 1999. A transmission-constrained unit commitment method in power system scheduling. *Decision Support Systems*, january, pp. 297-310.

VAN DEN BERGH, K., DELAURE, E. & D'HAESSELLER, W., 2014. *DC power flow in unit commitment models*, KU Leuven Energy Institute: s.n.

Wong, S. & Fuller, J. D., 2007. Pricing energy and reserves using stochastic optimization in an alternative electricity market. *IEEE Transactions on Power Systems*, 22(2), pp. 631-638.

WOOD, A. J. & WOLLENBERG, B. F., 1996. *Power Generation, Operation and Control*. s.l.:s.n.

WRIGHT, W. J. & JOHNSON, R. C., 1971. Large scale hydro-thermal unit commitment-method and results. *IEEE Transactions on Power Apparatus and Systems*, Volume PAS-90, pp. 1373-1384.